

TMAL06 Final Report

UAV for Medical Payloads

Meet Akhil Kumar Agrawal, meeag462

Rakesh Nagaraja, rakna614

Rohit Raja, rohra521

Yuvarajendra Anjaneya Reddy, yuvan983

Academic supervisor: Alejandro Sobron

External supervisor: Christopher Jouannet

Examiner: David Lundström

Contents

| | | |
|----------|--|-----------|
| 1 | Introduction | 1 |
| 1.1 | Project Description and Background study | 1 |
| 1.2 | Preliminary mission requirements | 2 |
| 1.3 | Mission profile | 2 |
| 2 | Background Studies | 3 |
| 2.1 | Competitor analysis | 3 |
| 3 | Concept Generation | 5 |
| 3.1 | Morphological matrix | 6 |
| 3.2 | Developed concepts | 6 |
| 3.3 | Summary of developed concepts | 10 |
| 4 | Concept Selection | 11 |
| 4.1 | Analysis of generated concepts | 11 |
| 4.2 | Scoring matrix | 12 |
| 4.3 | Finalizing the concept | 13 |
| 4.4 | Quality Function Deployment | 16 |
| 5 | Detailing of Selected Concept | 17 |
| 5.1 | Constraint diagrams | 17 |
| 5.2 | Selection of design point | 20 |
| 5.3 | Derived specifications from the design point | 22 |
| 5.4 | Airfoil selection | 22 |
| 5.5 | Weight estimation | 23 |
| 5.6 | Propulsion system and Battery selection | 25 |
| 5.6.1 | Powerplant | 25 |
| 5.6.2 | Propellers | 26 |
| 5.6.3 | Electronic speed controller | 26 |
| 5.6.4 | Battery | 26 |
| 5.7 | Tail sizing | 27 |
| 5.8 | Aerodynamic centre, Neutral point and CoG estimation | 28 |
| 5.9 | Control surfaces sizing | 30 |
| 5.10 | Miscellaneous systems in the UAV | 31 |
| 5.11 | Range and Endurance as a function of cruise speed | 32 |
| 5.12 | Power required as a function of cruise speed | 34 |
| 5.13 | Drag Polar | 35 |
| 5.14 | Specific Excess Power | 36 |
| 5.15 | V-n Diagram | 36 |
| 5.16 | Parachute Sizing | 36 |
| 6 | Final Results | 38 |
| 7 | Discussion and Conclusion | 40 |

1 Introduction

Humans, the most intellectual ones, tend to keep up this title by exploring unknown dimensions of known things. Specifically engineers thrive days and nights finding optimal solutions to the day to day problems. Flying was one such greater achievements of mankind. Unmanned Aerial Vehicles, a common name for Remotely Piloted Aircraft (RPA) are on their way of revolutionising modern day means of transport in logistics. The term unmanned aerial vehicle(UAV) was first coined in the 1980s to describe autonomous, or remotely controlled, multi use aerial vehicles that are driven by aerodynamic forces and are capable of carrying a payload.[1] The versatile capabilities and dynamic features of UAVs turn them to be potential game changers.

UAVs, in this fast operating, time conscious era have many civil applications. They are being used for agricultural purposes, development aid work, military purposes (reconnaissance), aerial survey and photography, logistics transportation and so on. Logistics can be efficiently transported to and from point A to point B, by employing the unmanned aerial vehicles, saving a lot human effort, operational time and resources. Transportation of medical goods is one such area in which UAVs are expected to have greater potentials.

Unmanned aircraft vehicles (UAVs) have greater advantages in the field of logistics transportation's compared to the conventional modes of transport in terms of man power used, infrastructure required, turn around time, safety concerns and accessibility to remote locations. UAVs have had a rapid escalation in manageability and affordability, which can be exploited in healthcare.[2]

1.1 Project Description and Background study

This project aims on designing a logistics UAV for transportation of medical goods. The term medical goods here mainly refers to blood packets, medicines and vaccinations. The need for medical attention in remotely accessible parts of the world at times is very crucial. There are many hurdles that one has to encounter to transport the medical goods to such remotely accessible places if conventionally transported by road or manned aircrafts. These are neither economically efficient nor highly reliable in geographically challenged areas.

Generally medical goods like the blood packets, laboratory samples and vaccines weigh between 0.5 - 4 kilograms, but are highly fragile in nature and have very limited shelf life unless they are stored in controlled environments. UAVs can be effectively put into use here. UAVs are capable of delivering goods safely, quickly, and economically across both accessible and inaccessible terrain in the rural areas of under developed countries. These UAVs may be manually controlled or pre-programmed to fly in specific routes or patterns.

In this project the UAV is designed to serve in the rural areas of African re-

gions like Tanzania, Rwanda and Juma island. Particularly focusing on Juma Island in Mwanza region, a landmass cut off from the mainland, where the world's second largest freshwater, Lake Victoria obstructs the laying of roads for conventional transportation. Mwanza region is located in the extreme northern quarter of mainland Tanzania, bordering Lake Victoria, and includes more than 86 inhabited islands in Lake Victoria. The whole Mwanza Region has 286 health facilities spread over the area.[3] These health facilities receive their inventory from the Mwanza city. This Juma island is 20.2 km away from the main city. The UAV would be a very apt means of transport here to deliver medical tissues (laboratory samples), blood sachets, vaccines to-and-fro from the Mwanza city to Juma island. The rapid delivery of the medical needs could save lives and also minimise the outbreak of deadly communicable diseases.

1.2 Preliminary mission requirements

In order to carry out the mission, that is to deliver medical supplies and cargo to the remotely accessible places, it is necessary to have some preliminary estimates on the purpose and functions of the UAV. Considering the above mentioned situation, the mission requisites are:

- Range : 120 kilometres
- Payload capacity : 2-4 kilograms
- Cruise speed : 100-150 kmph
- MTOW : 15 kilograms
- Propulsion : Electric motor with propeller
- Service ceiling : 2 kilometres
- Take off : Catapult
- Landing mechanism : Arrestor hook / Belly landing

1.3 Mission profile



Figure 1: Mission profile depiction

2 Background Studies

2.1 Competitor analysis

A background study is performed on few of the benchmark UAV companies actively working on the transport of the medical devices to the inhospitable regions, to get an idea of the preliminary requirements for the conceptual design. The transported medical devices include external fixator devices, automatic defibrillators, combat gauze, torquinet, blood packets, and also food in emergency situations. Few researched companies along with their operations are observed as follows:

- Zipline - The company operates a fleet of drones to deliver blood products on a national scale to remote areas of Rwanda and Ghana. The UAV is a fixed-wing battery-powered, with a service radius of 80 km for delivering a payload of 1.8 kg with average delivery time of 30 minutes. The operated UAV can be observed in Fig. 2.



Figure 2: Zipline UAV

- Swoop Aero - The company provides essential medical services to the inhospitable regions of Vanuata. The UAV is a fixed-wing battery-powered. The operated UAV is shown in Fig. 3.



Figure 3: Swoop aero UAV

- Wingcopter - The company provides the customers with a range of services like 3-D mapping, monitoring, delivering, and some custom operations to remote health facilities. The UAV operates for a range of 100 km with a speed of 240



Figure 4: Wingcopter UAV

kmph by implementing a Vertical Take-Off Landing (VTOL) mechanism for a payload of 6 kg. The operated UAV is shown in Fig. 4.

- Latitude Engineering - The company is developing a concept UAV for long endurance operations using a VTOL mechanism. The concept is being developed for 15 hours of endurance with a fixed-wing configuration supporting a payload of 10 kg at a max speed of 120 kmph. The concept UAV is shown in Fig. 5.



Figure 5: Latitude Engineering UAV

- Delivery Future - This is a pilot project in joint association by DHL, GIZ and wingcopter to develop a UAV for delivering medicines to remote areas. The UAV uses a fixed-wing configuration, and is designed to carry a payload of 4 kg upto a range of 65 km. The developed UAV can be seen in Fig. 6.



Figure 6: Delivery Future UAV

3 Concept Generation

The design process is a multidisciplinary principle. According to M.P. Weiss and Y. Gilboa, “Conceptual design is considered as the most important step in the design of a new product. There the performance of the product is generated and about 75p.c of the life cycle cost (LCC) is committed.” [4]

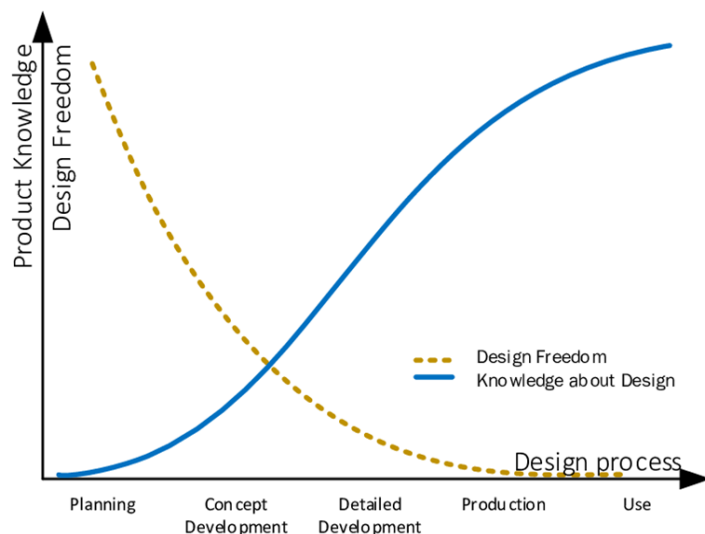


Figure 7: Design paradox

Figure 7 shows the design paradox for a product. Initially during the planning phase, the engineer has very little knowledge about the design end product, which provides him a huge design space freedom to explore out various possible means. and the decisions made here are based on less information compared to the decisions made in the later stages. As the design process advances with time, the product knowledge curve rises gradually as the design freedom curve falls yielding much constrained design space. The correction of the mistakes made in the conceptual design phase during the final design stages would be a herculean task for the designer with limited design freedom as bonus.

Henceforth, the conceptual design phase of design process has greater after effects if not executed properly. In this assignment, this process is carried out systematically in order to save time and not to lack the vital factors influencing the design. The conceptual design of the Medico- fly UAV is started by searching for inspirational aircraft designs or concepts that would serve our required aim. The conventional aircraft design techniques from Roksam and Raymer are based on empirical data of the existing aircrafts, which cannot be fully applied to our case. The main aspects that were considered to filter out the concepts are payload carrying capability, ease of manufacturing, robustness and simplicity in terms of aerodynamic technicalities.

3.1 Morphological matrix

To carry out the design process in systematic manner, the design space was exploited by creating a Morphological matrix of the functions along with the means to achieve the functions. The morphological matrix provides a visual insight on the product functionality and lets the designer have numerous alternative means and combinations of achieving the end functionality[5]. Also, the matrix provides us with a vast design space to explore into and choose a concept based on individuality. The number of possible combinations generated from the morphological matrix is calculated as $(Functions)^{means}$. Hence, the matrix provides us with a design space of about 20736 combinations to explore into. Here, an example for a concept generation is displayed in Fig. 18.

| COMPONENT/CRITERIA | Option 1 | Option 2 | Option 3 | Option 4 |
|--------------------|---------------|----------------|-----------------|-----------------------|
| FUSELAGE SHAPE | Circular | Rectangular | Elliptical | Irregular |
| WING | Rectangular | Elliptical | Tapered | Swept |
| WING POSITION | High wing | Mid wing | Dihedral | Anhedral |
| TAIL | Conventional | T-tail | H-tail | Butterfly tail |
| PROPELLION | Electric | Combustion | Hybrid | Solar powered |
| ENGINE PLACEMENT | Nose | Tail | Wing | Blended in wings/tail |
| ENGINE NUMBER | 1 | 2 | 3 | 4 |
| CONTROLS | Conventional | Ruddervators | Canards | Dorsal/Ventral fin |
| MATERIAL | Aluminium | Epoxy | Carbon fibre | Fibre glass |
| PAYOUT POSITION | Nose | Tail | Inside fuselage | Under fuselage |
| TAKE OFF | Hand thrown | Catapult | Wheels-runway | VTOL |
| LANDING | Belly landing | Arrester hooks | Wheels-runway | VTOL |

Figure 8: Morphological matrix with an example path of means

Figure 18 represents the aircraft morphological matrix for aircraft design. Here the components column indicate the functions and other columns represent the means to achieve the respective function.

Four different concepts were developed, which had their own pros and cons but ultimately served the end function of delivering the medical cargo. Initially the concepts were sketched down on blank sheets without any dimensions, but later on were designed in CATIA V5 software. The new generated concepts can be observed in the following sub-section.

3.2 Developed concepts

- Concept 1: The developed concept can be observed from Fig. 9 and Fig. 10, respectively.

The pros for concept 1 can be observed as follows,

- Elliptical wing, efficient spanwise lift distribution

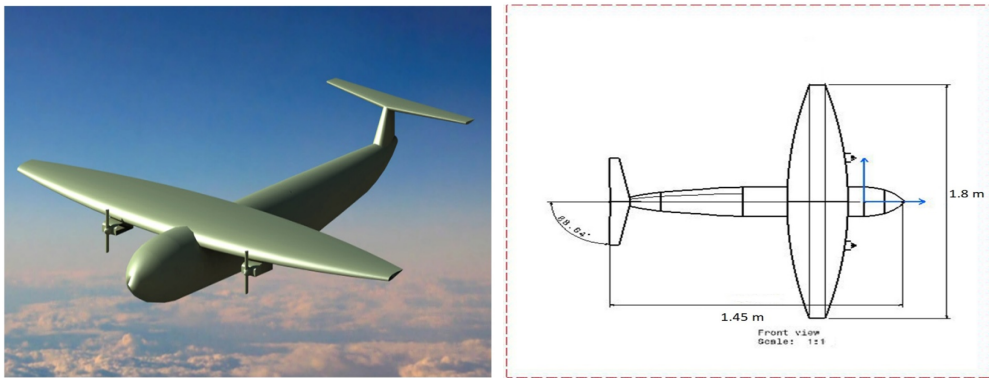


Figure 9: Isometric and top view of concept 1

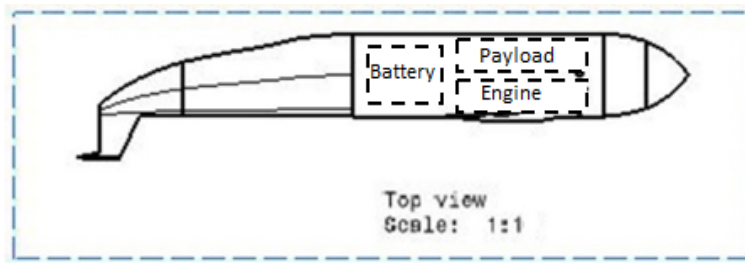


Figure 10: Side view of concept 1

- T-tail gives more leverage and low weight

The cons for concept 1 can be observed as follows,

- Chances of deep stall and tail blanking at high AoA
- Manufacturing difficulties

- Concept 2: The developed concept can be observed from Fig. 11 and Fig. 11, respectively.

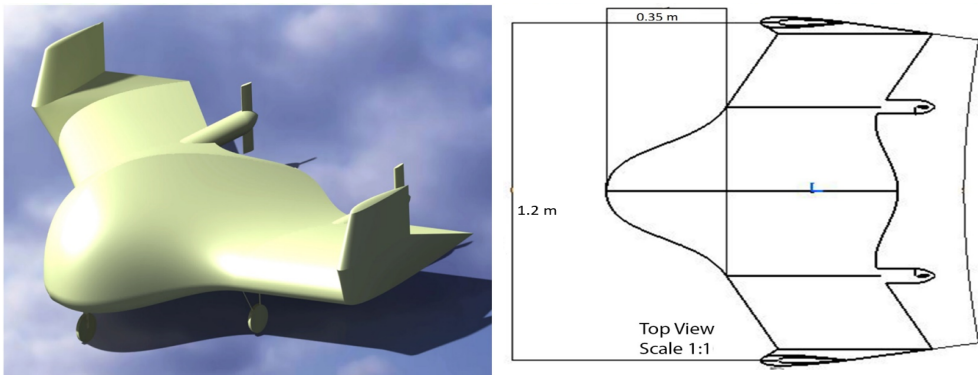


Figure 11: Isometric and top view of concept 2

The pros for concept 2 can be observed as follows,

- Single structure with proper load distribution
- High internal volume for cargo/payload

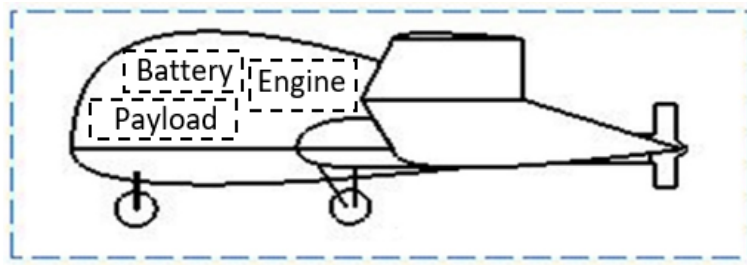


Figure 12: Side view of concept 2

The cons for concept 2 can be observed as follows,

- Low stability for precision transport
 - Aerodynamically complex
- Concept 3: The developed concept can be observed from Fig. 13 and Fig. 14, respectively.

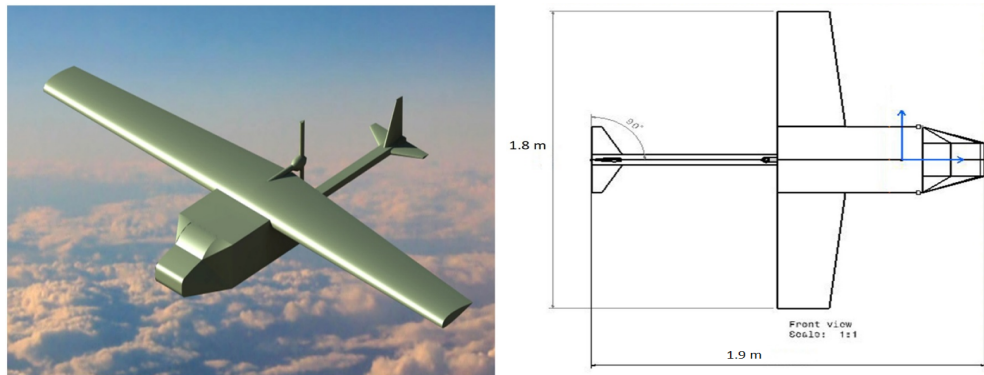


Figure 13: Isometric and top view of concept 3

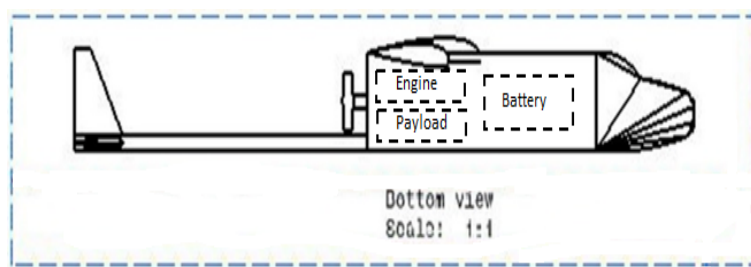


Figure 14: Side view of concept 3

The pros for concept 3 can be observed as follows,

- Detachable wing
- Tapered wing

The cons for concept 3 can be observed as follows,

- Manufacturing complexities
- Moderate take-off performance

- Concept 4: The developed concept can be observed from Fig. 15 and Fig. 16, respectively.

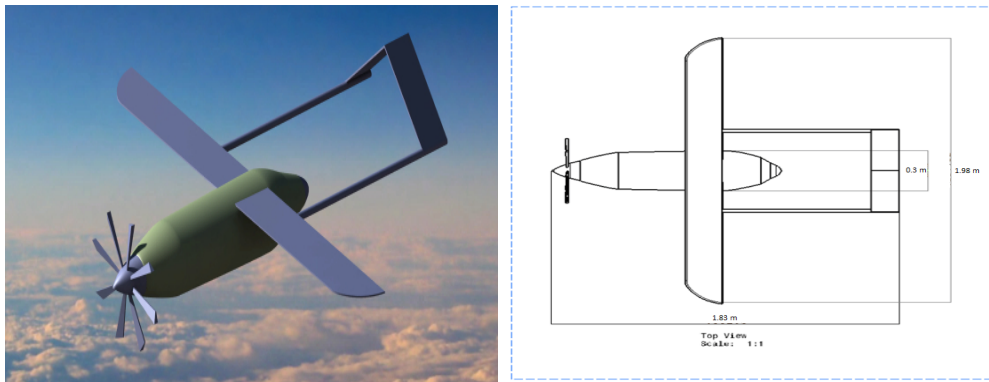


Figure 15: Isometric and top view of concept 4

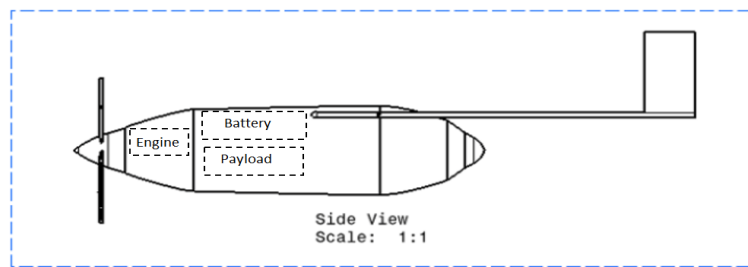


Figure 16: Side view of concept 4

The pros for concept 4 can be observed as follows,

- Lower Stall Speed
- Fewer Control Surfaces

The cons for concept 4 can be observed as follows,

- Higher Induced Drag
- Failure of V-Tail in case of malfunction

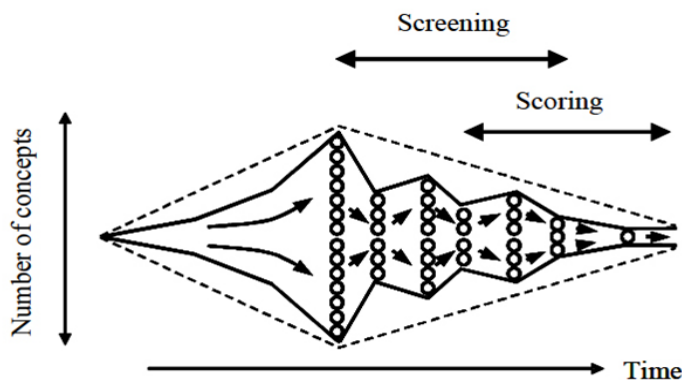
3.3 Summary of developed concepts

| Concept | Concept 1 | Concept 2 | Concept 3 | Concept 4 |
|-------------------|---------------|--------------|-----------------|------------------|
| Wing Type | Elliptical | Blended Wing | Tapered Wing | Rectangular Wing |
| Wing Span | 1.8 m | 1.2 m | 1.8 m | 1.98 m |
| Fuselage Length | 1.45 m | 1 m | 1.9 m | 1.83 m |
| Propulsion | Electric | Electric | Electric | Electric |
| Engine Placement | Wing mounted | Wing mounted | Blended in Wing | Nose mounted |
| Number of Engines | 2 | 1 | 1 | 1 |
| Take-Off | Catapult | Landing Gear | Catapult | Catapult |
| Landing | Belly Landing | Landing Gear | Arrester Hooks | Arrester Hooks |

4 Concept Selection

Concept selection is a crucial phase of concept design. So, a more careful concept phase selection process is opted for, using the concept phase diagram developed by Ulrich and Eppinger. According to the Ulrich and Eppinger, the initial phase of a concept is divergent in nature in comparison to time, since a lot of design freedom exists to explore the design space available. Afterwards, it follows a convergent nature with time, since after the exploration of the design phase, the concept phase of the product is screened through phases like system-level design, detail design, testing and refinement, followed by the mass production of the product. After generating concepts one has to be logical in selecting the best concept, which involves analyzing the pros and cons of the generated concepts by each group member, and screening unwanted parts with the help of a scoring matrix criterion.[6]

Concept generation phase is divergent in nature as many ideas are pooled in, contrarily this selection phase is much of convergent nature, as presented in Figure 17



The concept phase according to Ulrich & Eppinger.

Figure 17: Screening and scoring curve nature

The concepts are graded and compared against each other by their ability to fulfill the required task in an efficient manner. This is discussed in further subsections.

4.1 Analysis of generated concepts

The four concepts generated are unique in their own ways and are better only in certain things. A closer study was carried in order to rule out the misfits that do not perform efficiently for the aim of this project. Aerodynamic performance and simplicity of the concept were put on high priority during this process. The discussions regarding the implemented sub concepts are being noted as follows:

- The main objective behind the spitfire inspired design (Concept 1) is that, to reduce aerodynamic complexities and be capable of STOL (Short Take-off and Landing). Pull propeller at the nose of fuselage for thrust can be considered as an alternative. Fuselage is of airfoil shape to add up the lift generation.

- Blended wing comes with huge complexities compared to the other generated concepts from manufacturing point of view and aerodynamic performance view.
- V-tail has smaller size, less wetted area, less drag and fewer control surfaces which can be advantageous here. But redundancy is what matters here, where the V-tail is poor.
- Winglets aid in reducing trailing vortex drag, which increases lift generation, which can be considered during high speeds though it is irrelevant here.
- Joint wing configuration helps in reducing the wing span, but a catapult mechanism requires small and compact UAV for ease of deployment. Hence joint wing cannot be taken into consideration here.
- High wings have comparatively better lateral stability than the medium or low wings. As the UAV designed is to be hand launched or catapult launched, UAV has to have greater stability's at low speeds. So high wings are the best option here.
- Wing sweep was not considered as this feature is only useful for high speed flights. The UAV in this project would b designed to fly at comparatively lower speeds.
- The optimal design would be elliptical to have uniform span wise distribution of lift with lowest possible induced drag possible. But elliptical wing has manufacturing complexities, so here the wing is almost a straight taper with taper ratio around 0.3-0.4.
- However, uniform lift distribution allows the aircraft to stall much earlier than the traditional thing, which makes us to worry more about washout, that even increases the error.
- Dihedral increases the stability, but in turn decreases the effective span of the aircraft, which is highly risky here.
- Tilt rotor was excluded due to its complexities with servo mechanisms and due to the increased weight of additional servos.

4.2 Scoring matrix

The scoring matrix is being developed to assess the criterion for the concept selection process, and is graded on few important parameters presented in the matrix 18. The scoring criteria of the generated four concepts are briefly stated below :

- Aerodynamics - Aerodynamically efficient wings, in terms of lift distribution over the wing span, manufacturing complexities and placement of the wings (high or low position)
- Propulsion - This parameter is graded for different concepts, based on the effect of placement of propulsion system in relevant position, on the overall efficiency of the UAV.

- Structural endurance - The main concern here is the rigidity of the structure and capability to produce less drag (interference drag).
- Manufacturability - Manufacturing ease is the top priority here. Manufacturing a rectangular fuselage is less risky job compared to a blended wing structure.
- Performance - Aerodynamic performance parameters like L/D ratio, maneuvering, control surfaces simplicity, redundancy, versatility were considered.
- Balancing - This parameter was based on the sensitivity of design to the shifts in the centre of gravity and aerodynamic centre on making any important structural placements like changing the engine mount position, battery position, payload placement position and so on.
- Maneuverability - Based on very crude estimation of control surface deflection and the ability of the aircraft to be in trimmed condition when maneuvers are performed the grading were provided.
- Cross-wind operations - The grading was done based on the extent to which the generated design concept would overcome the crosswinds condition.
- Reliability and Portability - Storage and maintenance in terms of cost of operation and initial cost of production were considered here.

Based on the above-mentioned parameters, the generated scoring matrix along with the score scaling can be observed from Fig. 18.

| Parameter | Concept 1 | Concept 2 | Concept 3 | Concept 4 |
|----------------------|-----------|-----------|-----------|-----------|
| Aerodynamics | 4 | 4 | 2 | 4 |
| Propulsion | 4 | 2 | 2 | 4 |
| Structural endurance | 3 | 4 | 4 | 2 |
| Manufacturability | 2 | 1 | 3 | 1 |
| Performance | 3 | 2 | 3 | 3 |
| Balancing | 4 | 1 | 4 | 4 |
| Maneuverability | 3 | 1 | 3 | 2 |
| Cross-Wind operation | 4 | 2 | 3 | 1 |
| Reliability | 3 | 1 | 4 | 2 |
| Portability | 2 | 2 | 3 | 2 |
| | 32 | 20 | 31 | 25 |

| Legend | |
|--------|-----------|
| 1 | Poor |
| 2 | Average |
| 3 | Good |
| 4 | Excellent |

Figure 18: Scoring matrix for screening out the generated concepts

4.3 Finalizing the concept

Here, it can be observed from Fig. 18 that, concept 1 and concept 3 have an almost equal scoring being assigned. Hence, a final concept will be developed taking into consideration the pros of both the concepts, and further tasks would be performed. The finalized concepts 1 and 3 can be observed from Fig. 19.

Hence, it can be observed from Fig. 19 that since two concepts are selected, a blend of both the concepts is to be developed with pros from both the concepts.

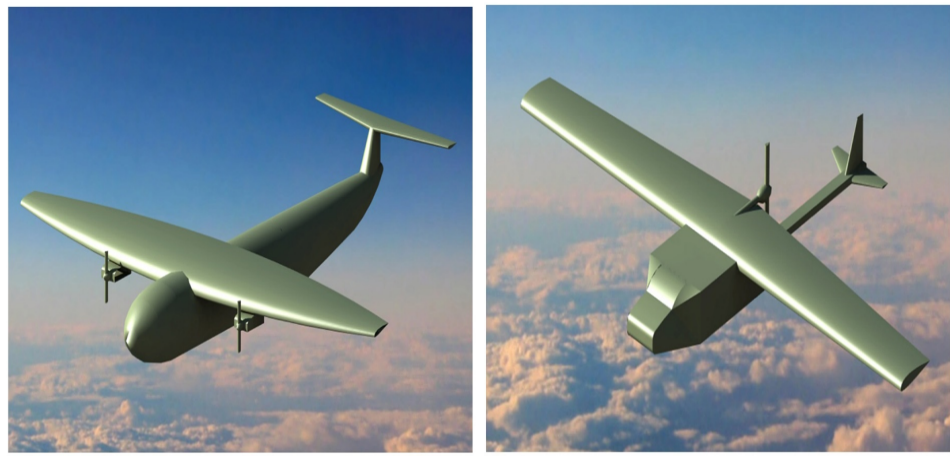


Figure 19: Selected concepts

The newly developed concept can incorporate the advantages of both the concepts like taking into consideration the streamlined fuselage from concept 1, which can help in reducing the drag on the UAV and can have a more streamline flow over the fuselage. Another possible modification would be the mounting of the wings to a high-wing mount configuration, which would help in the landing of the UAV, since a belly-landing approach is being implemented here. Also, to assist the propulsion, the propeller are wing-mounted so the propellers are damaged while landing. Since a high-wing configuration is used, a conventional tail empennage can be opted for so that an undisturbed flow over the tail is attained, thereby generating less interference drag. Also, the internal components like the payload bay, battery and the motor can be mounted accordingly to balance the UAV. The 2d drawing with the dimensions can be observed from Figure 20, while the payload orientation and the side view of the UAV can be observed from Figure 21.

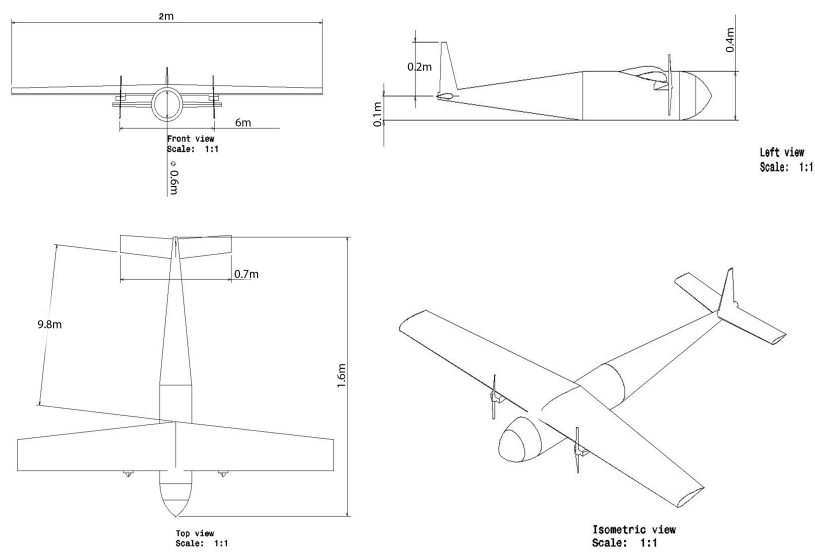


Figure 20: The 2d drawing of the selected concept

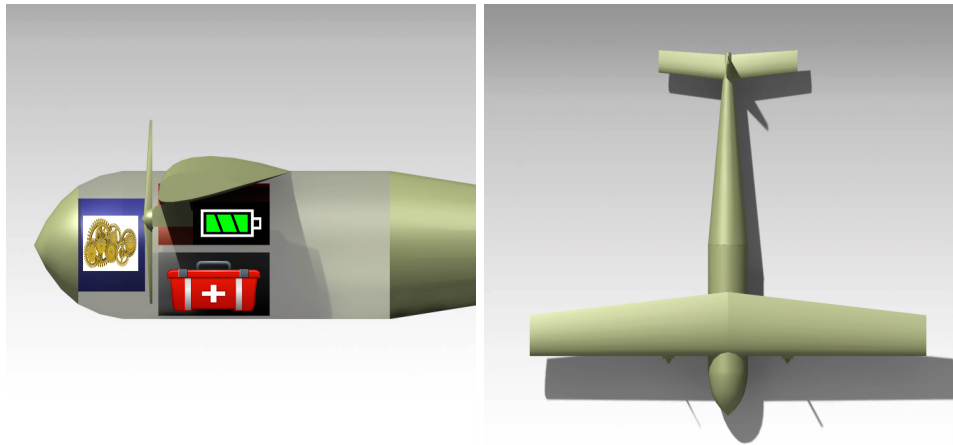


Figure 21: Payload orientation and the top-view of the new concept

Also, a pneumatic catapult launcher was designed, and can be observed from Figure 22.

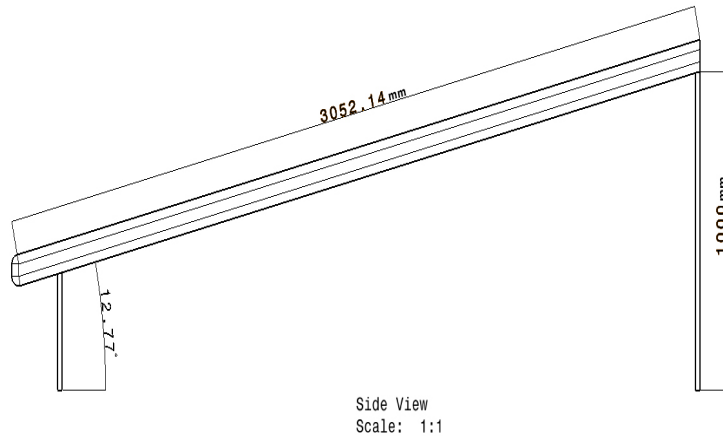


Figure 22: Side view of the designed launcher

It can be observed from the launcher design that a rail length of around 3 m was opted for with a launching angle of 12.7° , since most of the UAV launches occur at around 12° . Also, the height of the rail can be adjusted by varying the launching angle. Also, to get the required rate of climb (ROC) during strong head-winds or cross-wind conditions, the launching angle can be varied accordingly for an optimum climb. The launcher is designed such that the legs are foldable, as well as detachable for quick and proper storage when not in use.

The stall speed for the UAV is 20 m/s, so for a stall-free launch, the launching velocity should be higher than the launching velocity. Hence, for a launching velocity higher than the stall speed, a launching pressure of 10 bar, for a plane mass of 15 kg, is required from the pneumatic cylinder, as observed from Figure 23.[7]

| Pressure (bar) | Plane mass (kg) | | | | | |
|-----------------------|-----------------|------|------|------|------|------|
| | 10 | 15 | 20 | 30 | 40 | 45 |
| Launch velocity (m/s) | | | | | | |
| 5 | 18,4 | 15,1 | 13,1 | 10,7 | 9,4 | 8,9 |
| 6 | 20,2 | 16,5 | 14,3 | 11,7 | 10,3 | 9,7 |
| 7 | 21,8 | 17,9 | 15,5 | 12,6 | 11,2 | 10,5 |
| 8 | 23,3 | 19,1 | 16,5 | 13,5 | 12,0 | 11,2 |
| 9 | 24,8 | 20,3 | 17,6 | 14,3 | 12,7 | 11,9 |
| 10 | 26,1 | 21,3 | 18,5 | 15,1 | 13,4 | 12,6 |
| 11 | - | 22,4 | 19,4 | 15,8 | 14,0 | 13,2 |
| 12 | - | 23,4 | 20,3 | 16,5 | 14,6 | 13,8 |
| 13 | - | 24,3 | 21,1 | 17,2 | 15,2 | 14,3 |
| 14 | - | 25,3 | 21,9 | 17,9 | 15,8 | 14,9 |
| 15 | - | 26,1 | 22,7 | 18,5 | 16,4 | 15,4 |
| 16 | - | - | 23,4 | 19,1 | 16,9 | 15,9 |

Figure 23: Launcher specifications

4.4 Quality Function Deployment

A Quality Function Deployment (QFD) is developed to translate the customer requirements to the engineering characteristics of the company, to make it easier for the employees to understand what the customer actually wants and demands for. QFD is also employed into businesses to come up with some cost cutting solutions, as a communication tool between various departments, and also in reducing the product development time.

Also a grading scale of 1/3-least importance, 1-important, 3-significant importance, 9-extremely important, is adopted to grade the customer requirements into the QFD matrix.

| | Weight | Drag | Cruise speed | Range | Battery efficiency | Structural stability | Payload | Maneuverability | Rate of climb | Service ceiling | Maximum G's | Manufacturing cost | Ease of operation | Reliability | Maintainance | Total |
|-------------|-----------------------------|------|--------------|-------|--------------------|----------------------|---------|-----------------|---------------|-----------------|-------------|--------------------|-------------------|-------------|--------------|-------|
| Efficiency | Weight | 9 | 3 | 3 | 1/3 | 9 | 3 | 9 | 9 | 3 | 9 | 1/3 | 3 | 1/3 | 1/9 | 61.11 |
| | Drag | 1/9 | 1 | 3 | 1/3 | 9 | 1/3 | 9 | 3 | 3 | 3 | 1 | 3 | 1 | 1/9 | 36.89 |
| | Cruise speed | 1/3 | 1 | 1/3 | 1/3 | 3 | 1 | 9 | 3 | 1/3 | 9 | 1 | 3 | 1/3 | 1/9 | 31.78 |
| | Range | 3 | 3 | 3 | 1/9 | 1 | 1/3 | 1/3 | 3 | 3 | 9 | 1 | 3 | 1 | 1/9 | 50.22 |
| | Battery efficiency | 9 | 3 | 3 | 9 | 1 | 1/3 | 1/3 | 3 | 1 | 9 | 9 | 3 | 9 | 3 | 62.67 |
| | Structural stability | 9 | 3 | 3 | 1/3 | 1/3 | 3 | 9 | 1 | 1 | 9 | 3 | 3 | 9 | 3 | 56.67 |
| Performance | Payload | 3 | 1/3 | 3 | 9 | 3 | 1/9 | 1/3 | 1/3 | 1/3 | 1/3 | 1/6 | 1/6 | 1 | 1/9 | 21.22 |
| | Maneuverability | 1/9 | 3 | 1/9 | 1/9 | 1/9 | 3 | 3 | 1/3 | 1/3 | 1 | 1/3 | 1/3 | 1/3 | 1/9 | 12.22 |
| | Rate of climb | 1/9 | 1/3 | 1/3 | 1/3 | 1/9 | 1/3 | 3 | 1 | 1 | 1/3 | 1 | 1/3 | 1/9 | 1/9 | 8.667 |
| | Service ceiling | 3 | 1 | 1/3 | 9 | 1/3 | 1/3 | 3 | 1 | 3 | 1 | 1/3 | 3 | 1 | 1/9 | 26.44 |
| | Maximum G's | 1/9 | 1/3 | 1/9 | 1/9 | 1 | 3 | 3 | 3 | 1/6 | 1 | 1/3 | 1 | 1/3 | 1/9 | 13.61 |
| | Manufacturing cost | 3 | 1 | 1 | 1 | 1/3 | 3 | 3 | 1/9 | 1/9 | 1 | 1 | 1 | 3 | 18.67 | |
| Others | Ease of operation | 1/3 | 1/3 | 1/3 | 1/3 | 3 | 1 | 3 | 1 | 1 | 1 | 1 | 1 | 1/3 | 1/3 | 13.33 |
| | Reliability | 3 | 1/3 | 3 | 1 | 1/9 | 3 | 3 | 3 | 3 | 3 | 1 | 9 | 3 | 3 | 38.44 |
| | Maintainance | 1/3 | 1/3 | 1/6 | 1/3 | 1 | 3 | 1/3 | 1/3 | 1/6 | 1/3 | 1 | 3 | 3 | 1 | 13.67 |

Figure 24: QFD matrix with scoring for the performance parameters of the final design concept

It can be observed from Figure 24 that battery efficiency has been rated the highest score in all the aspects, and it also makes sense to have a good and efficient battery back-up since our main aim of the project is to implement a robust UAV for delivering medical devices to inhospitable regions with remote access. Another highlighting important parameter by the customer is the weight of the UAV, which indirectly affects the required power for launching. Having a lighter UAV, would help us to launch in a faster way in case of emergencies.

5 Detailing of Selected Concept

5.1 Constraint diagrams

Constraint diagrams are the critical evaluation figures of the performance of the aircraft during the conceptual design phase. It mainly involves two parameters namely, power to weight ratio (P/W) and wing loading (W/S). The constraint diagram provides the primary advantage to the designer to assess the required propulsion power plant and wing area to complete a particular mission.

In the constraint diagram, the relative significance of performance constraints on the design are plotted in the design space, a 2-D graph of power loading vs wing loading. [8]. The space above the constraint curves in the graph is termed as the design space.

Constraint analysis is performed to effectively screen the choices of the many interrelated parameters that control the performance of the aircraft, and make appropriate choices such that the design fulfills the required capabilities of the mission. Constraint analysis provides ranges of values for an aircraft concept's take-off wing loading and takeoff power loading, which allow the design to meet specific performance requirements.

The idea behind an optimum design point in the constraint diagram is to minimize the power-loading, while maximizing the wing-loading at the same time. In the design space, any design point lying above the curve lies in the acceptable region (design space), a point below it lies in the unacceptable region, while a point lying exactly on the curve depicts the best or the desired design point from the customer's perspective.

A MATLAB code is implemented to solve and plot the necessary equations of the constraint diagrams. The important constraints considered here for the UAV design include a constant-velocity turn, rate of climb requirement, cruise airspeed, service ceiling, landing and take-off criteria. These performance characteristics of interest are written in the mathematical equations form, where the power loading (P/W) is expressed as a function of wing loading (W/S) i.e, $(P/W)=f(W/S)$, and can be observed from the following equations.

T/W for a level constant velocity turn

$$\frac{T}{W} = q \left(\frac{C_{D,min}}{W/S} + k \left(\frac{n}{q} \right)^2 \left(\frac{W}{S} \right) \right) \quad (1)$$

The above expression is used to determine the power loading (P/W) for a range of wing loading (W/S) to maintain a specific banking angle of 60 degrees to obtain a load factor of 2, at a cruise speed of 30 [m/s] for a 4000 ft flight altitude.

T/W for a desired rate of climb

$$\frac{T}{W} = \frac{V_v}{V} + \frac{q}{W/S} C_{D,min} + \frac{k}{q} \left(\frac{W}{S} \right) \quad (2)$$

Equation 2 represents the ROC equation, with a vertical speed of 10 ft/sec (3.048 [m/s]) at a cruise altitude of 4000 ft. As our fixed wing UAV correlates to a general aviation trainer aircraft, from the empirical data provided in [8] the value of $C_{D,min}$ is taken to be 0.027. And the lift induced drag factor, k is calculated by taking the aspect ratio to be 8 and Oswald's efficiency factor, $e = 0.81$. The reason for choosing AR = 8, is that the fighter planes have AR = 6-8 and glider planes have AR = 8-10. The mean of these extremes would provide us with a blend of characteristics of both the fighter and glider planes.

T/W for a desired cruise airspeed

$$\frac{T}{W} = qC_{D,min}\left(\frac{1}{W/S}\right) + k\left(\frac{1}{q}\right)\left(\frac{W}{S}\right) \quad (3)$$

The cruise speed equation (3) is used to get (P/W) ratios as the wing loading varies at an altitude of 4000 ft and cruise speed of 30 [m/s].

T/W for a service ceiling

$$\frac{T}{W} = \frac{V_v}{\sqrt{\frac{2}{\rho}\left(\frac{W}{S}\right)\sqrt{\frac{k}{3C_{D,min}}}}} + 4\sqrt{\frac{kC_{D,min}}{3}} \quad (4)$$

The service ceiling is set to be 4000 ft, viz approximately 1 km, a usual altitude for an UAV to fly so that it is insight of humans. The vertical speed of 10[ft/sec] is chosen here from the statistical data.

T/W for a desired take-off distance

$$\frac{T}{W} = \frac{V_{LOF}^2}{2gS_G} + \frac{qC_{D,TO}}{W/S} + \mu\left(1 - \frac{qC_{L,TO}}{W/S}\right) \quad (5)$$

Though the aim of this project is to develop a catapult launchable UAV, conventional take-off mechanism which involves ground run of 350 [m] is considered as an alternative. And the ground friction coefficient is taken to be 0.04 from the statistical data. And the landing constraint was constructed with the approach speed to be 20% greater than the stall speed.

Also the stall speed requirements are included in the constraint diagram, for the feasible maximum coefficient of lift that is possible to obtain with the installed wing.

The variables in the above equations are,

- S - reference wing area [m^2]
- T - Thrust [N]
- W - Weight [N]

- q - dynamic pressure at selected airspeed and altitude [N/m^2]
- $C_{D,min}$ - minimum coefficient of drag
- n - specific banking load factor (reciprocal of cosine of bank angle)
- k - lift induced drag factor
- V_v - vertical speed of the UAV [m/s]
- S_G - ground roll distance [m]
- $C_{D,TO}$ - coefficient of drag at the time of take-off
- $C_{L,TO}$ - coefficient of lift at the time of take-off
- g - acceleration due to gravity [m^2/s]
- V - cruise speed at steady state [m/s]
- V_{LOF} - lift-off speed [m/s]
- μ - ground friction constant

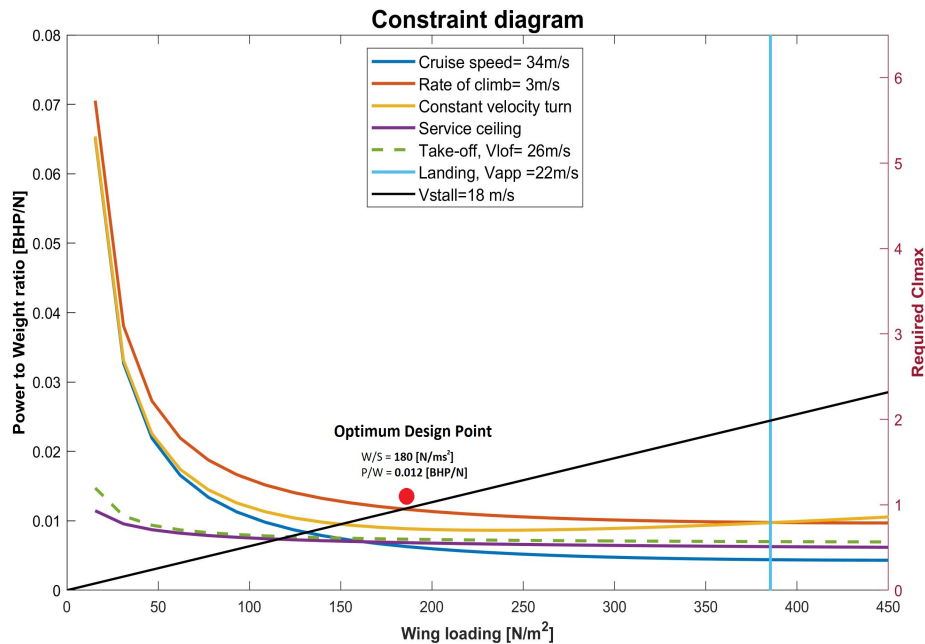


Figure 25: Constraint diagram with the optimum design point

Figure 25 shows the constraint diagram developed for the UAV with initial requirements that were stated. The red dot indicates the location of the optimum design point, and corresponds to a Power loading of 0.012 [BHP/N] and wing loading of 180 [N/m^2]. The design point very well fulfills all the required performance constraints within the reduced design space. From the stall limit constraint, it can be seen that the required maximum coefficient of lift is 0.95 corresponding to the optimum design point in order to meet the restriction.

5.2 Selection of design point

The design process is a multidisciplinary principle. The conceptual design process of the UAV is started by searching for inspirational aircraft designs or concepts that would serve our required aim. The main aspects that were considered to filter out the concepts were payload carrying capability, ease of manufacturing, robustness and simplicity in terms of aerodynamic technicalities. And the constraint diagrams were plotted by varying certain parameters to observe the variation of the design space. These plots are called as performance figures.

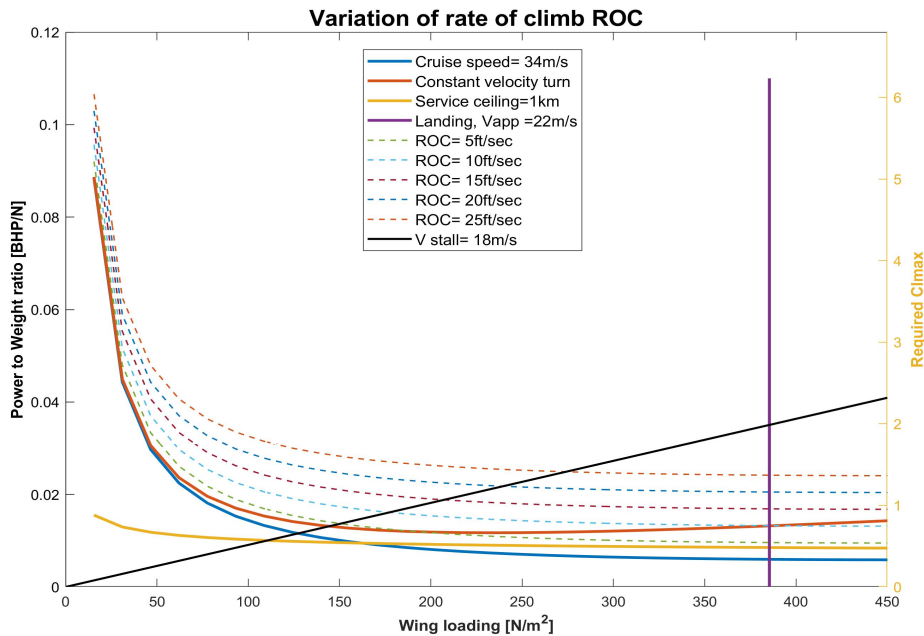


Figure 26: Constraint diagram with variation in climb rate (ROC)

From figure 26 it can be seen that as the rate of climb increases, the design space (the area above all the curves to the left of landing constraint) shrinks. Hence the optimum ROC was chosen to be 10 ft/sec.

Figure 27 shows the performance figure, as the cruise speed is varied from 30[m/s] to 45[m/s] in steps of 5[m/s]. Since the whole and sole aim of the UAV is to rush the medical goods to the needy situation, it is can be considered to increase the stall speed of the UAV without majorly affecting the other performance constraints. However, this has certain other effects which are not to be neglected. Keep this in mind, the cruise speed of the UAV is set to be 34[m/s], which could be subjected to changes later on.

Stall speed is one major constraint, which has its contribution from designing the shape and size of wing to cruising, landing and take-off. Figure 28 shows the variation in the design space as the stall speed is varied from 15-30[m/s] in steps of 5[m/s]. As the stall speed is increased the design space also increases. But increasing the stall speed means increasing the cruise speed, lift-off speed and approach speed. Also, the size of the wing is reduced so as to increase the stall speed. The chances of stalling the propulsion unit will be pretty much higher. However, general rule

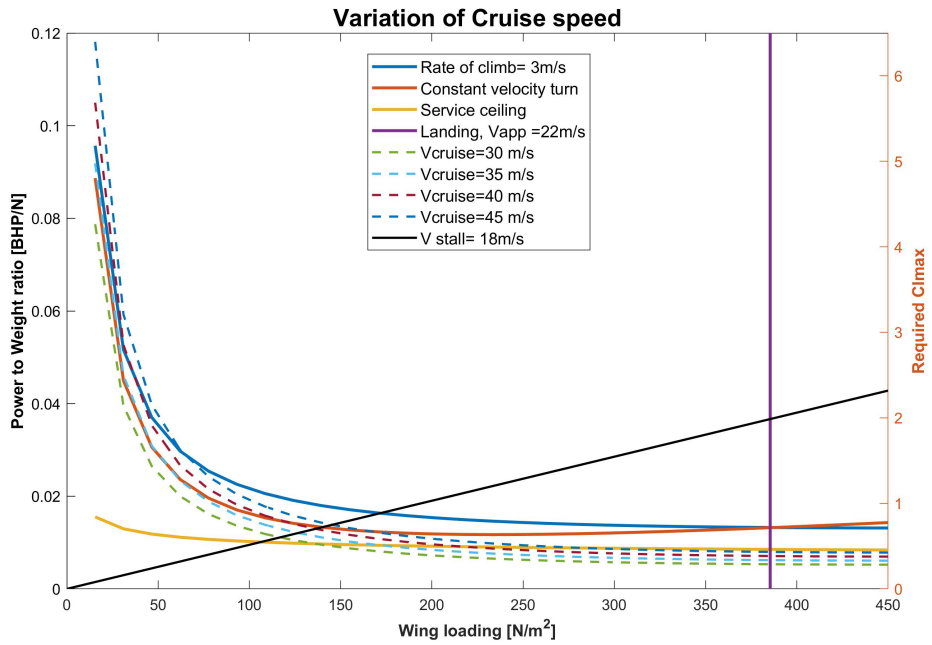


Figure 27: Constraint diagram with variation in Cruise speeds

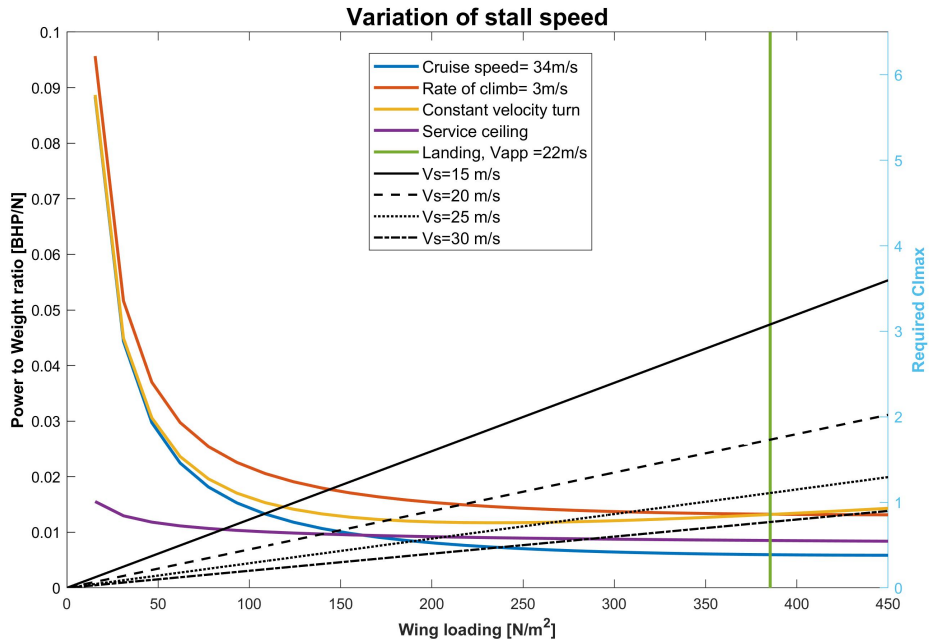


Figure 28: Constraint diagram with variation in Stall speeds

of thumb is to have the least possible stall speed. So, a stall speed of 18[m/s] was chosen here considering all the mentioned consequences.

5.3 Derived specifications from the design point

- Wing loading: **275** [N/m^2]
- Wing reference area (for MTOW=15[kg]): **0.5351** [m^2]
- Required power (for MTOW=15[kg]): **1.7143** [BHP]
- Wing span (for AR=8): **2.069** [m]
- Cruise speed: **120** [Km/hr]
- Maximum coefficient of lift: **1.3**
- Minimum coefficient of drag: **0.027**

5.4 Airfoil selection

Airfoil selection is an important criterion as it has passive effects on almost everything in an UAV. Maximum lift coefficient was the primary parameter considered for the crude study of selection of airfoils. Later on parameters like cruise lift coefficient, nature of drag polar, Pitching moment coefficient vs angle of attack curve, L/D ratios produced, stall angle, manufacturing ease and so on were taken into account to refine the study and screen the range of selected airfoils. The ability of the airfoil to have considerably lower drag in the cruise conditions is another much looked on property here, as the UAV is designed for and operates for a longer time in the cruising conditions.

Since the cruise speed is around 34 m/s , a low Reynolds number (Reynolds number calculated for cruise speed, altitude and wing chord of 250mm), high speed (for medical emergencies) airfoil was the requirement. Many similar UAVs were studied to get the statistical and historical trend of the airfoils employed and a few of them were assessed based on their aerodynamic efficiencies.

The short listed airfoils which were to be aerodynamically evaluated were NACA 23015, MH 104, Clark-Y, NACA 632(a)015 and Falcon. The drag polars, C_l vs alpha , C_d vs alpha and C_m vs alpha can be seen in Fig 29. It can be observed that the airfoil, NACA 23015 has comparatively higher coefficient of lift and also less pitching moment coefficient. Having a lesser C_m helps in reducing the volume of the tail. this in turn helps in the reduction of the weight of the aircraft. Also NACA 23015 has low drag response at Angle of attacks ranging from 5 to 12 degrees.

Finally, NACA 23015, a semi asymmetrical airfoil having a camber of 1.8pc and maximum L/D ratio of 72 at 10.5 degrees angle of attack, shown in Fig30 was chosen for the main wing. For the empennage section, there is no need for the generation of lift, hence cambered airfoil is not a requirement here. This greatly reduces the induced drag compared to the same thickness cambered airfoil. NACA 0012 shown in Fig 31airfoil was selected for the horizontal and vertical stabilizers, which has lower induced drag and is easier to build.

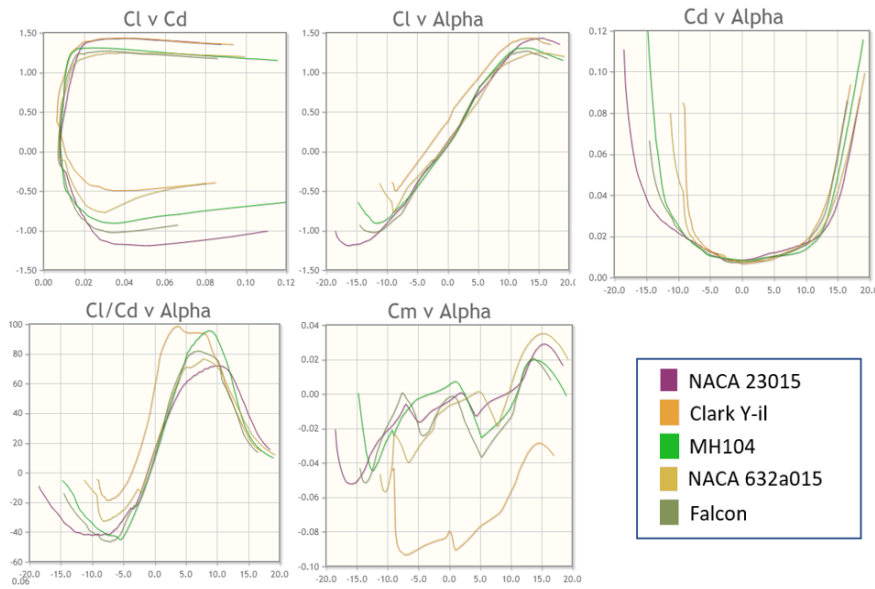


Figure 29: Airfoil aerodynamic evaluation graphs

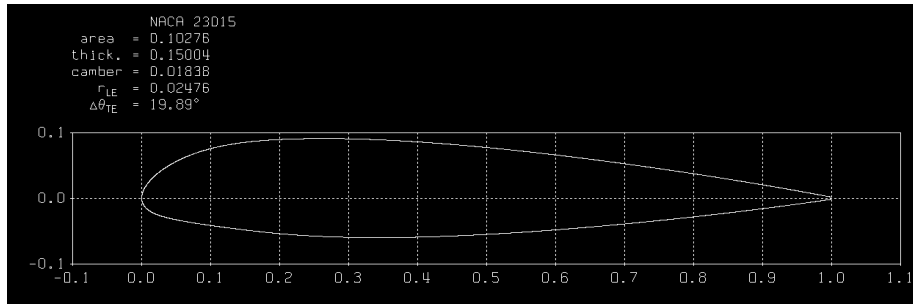


Figure 30: NACA 23015 having max thickness of 15pc at 30pc of chord and a camber of 1.8 pc

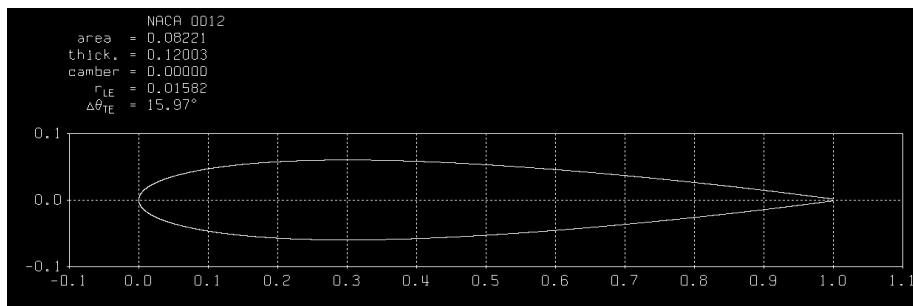


Figure 31: NACA 0012, symmetrical airfoil having max thickness of 12pc at 30pc of chord

5.5 Weight estimation

A main parameter in the weight estimation of a UAV is the gross weight W_0 , since it quantifies the weightage breakdown for the components of the UAV. Various weight estimation methods are available, of which, the statistical weight estimation

methods developed by Raymer, Nicolai[8] and Roksam [9] have been implemented here to get the initial estimated weight of the UAV. These weights are then used to determine the performance and dimensions of the UAV. The final gross weight of the UAV is calculated by summing up the component weights along with the payload.

A MATLAB code is implemented here to calculate the component weights.

Wing weight estimation by Nicolai,

$$W_W = 96.948 \left[\left(\frac{n_z W_0}{10^5} \right)^{0.65} \left(\frac{AR_W}{\cos^2 \Lambda_{c/4}} \right)^{0.57} \left(\frac{S_W}{100} \right)^{0.61} \left(\frac{1 + \lambda}{2(t/c)} \right)^{0.36} \sqrt{1 + \frac{V_H}{500}} \right]^{0.993} \quad (6)$$

Horizontal Tail weight estimation by Raymer,

$$W_{HT} = 0.016 (n_Z W_0)^{0.414} q^{0.168} S_{HT}^{0.896} \left(\frac{100(t/c)}{\cos \Lambda_{HT}} \right)^{-0.12} \left(\frac{AR_{HT}}{\cos^2 \Lambda_{HT}} \right)^{0.043} \lambda_{HT}^{-0.02} \quad (7)$$

Vertical Tail weight estimation by Nicoali,

$$W_{VT} = 98.5 \left[\left(\frac{n_Z W_0}{10^5} \right)^{0.87} \left(\frac{S_{VT}}{100} \right)^{1.2} \sqrt{\frac{b_{VT}}{t_{VT_{max}}}} \right] \quad (8)$$

Fuselage weight estimation by Roksam,

$$W_{FS} = (0.0025) K_{inlet}^{1.42} (q)^{0.286} W_0^{0.95} \left(\frac{l_{FS}}{d_{FS}} \right)^{9.81} \quad (9)$$

Electrical wire harness weight estimation by Roksam,

$$W_{CTRL} = (0.0268) W_0 \quad (10)$$

Fight control-system weight estimation by Roksam,

$$W_{CTRL} = (0.016) W_0 \quad (11)$$

Electronic propulsion systems weight estimation by Roksam,

$$W_{EPS} = \frac{P_{max}}{5} + (0.0654 P_{max}) + (0.0362 P_{max}) \quad (12)$$

Propulsion installation systems weight estimation by Roksam,

$$W_{PIS} = (1.03) N_{engines}^{0.3} \left(\frac{P_{max}}{N_{engines}} \right)^{0.7} \quad (13)$$

Instrumentation and avionics weight estimation by Roksam,

$$W_{Avionics} = N_{engines} (0.006) \left(\frac{W_0}{1000} \right) + (0.15 \left(\frac{W}{1000} \right)) + (0.012 W_0) \quad (14)$$

The calculated component-wise distribution obtained from the statistical method can be summarized in the following table,

Thus, on adding the weights, we obtain the initial estimated weight of UAV as **9.0535 kg**.

| Component | Estimated weight (kg) | Considered Method |
|--------------------------------|------------------------------|--------------------------|
| Wing | 1.538 | Nicolai |
| Fuselage | 0.981 | Roksam |
| Vertical tail | 0.0014 | Nicolai |
| Horizontal tail | 0.0853 | Raymer |
| Electrical wire harness | 0.4020 | Roksam |
| Flight Control System | 0.24 | Roksam |
| Electronic Propulsion System | 0.9228 | Roksam |
| Propulsion installation system | 0.3830 | Roksam |
| Avionics | 0.1824 | Roksam |
| Battery | 2.5 | Statistical data |
| Payload | 2 | Fixed |
| Total | 9.0535 kg | - |

5.6 Propulsion system and Battery selection

5.6.1 Powerplant

Aircraft propulsion plays a key role in designing a UAV for medical supplies as delivery time plays a vital role in establishing the Unique selling point. Several Propulsion configurations were considered before actually selecting the powerplant. Nose mounted and wing mounted engines were the most suitable options. But nose mounted configuration was ultimately ruled out because of low ground clearance due to belly landing. Hence, wing mounted configuration was selected.

The pivotal requirements of the propulsion system are unit weight and Maximum operating power. This enables the UAV to carry more payload, faster.

The required power to propel the UAV is 1.2783 kW which was determined from the Constraint Diagram. Hence, a motor with similar operating power was found: SII 3020-890KV (V2) by Scorpion®. Each motor is capable of producing close to 780 watts as maximum continuous power. But this is obtained at 100 p.c throttle setting. From various studies it is confirmed that running the electrical motors on 100 p.c throttle setting will lead to over heating issues and burn the windings and damage the interiors. Hence a throttle setting of 70-85 p.c is recommended. Hence two of these motors are required. A detailed specifications list of the motor can be seen in Fig. 33.



Figure 32: Scorpion SII-3020-890KV (V2) motor

Although the maximum power is much higher than the required power, it is

Specifications

| | | | |
|--------------------------|-------------------|------------------------|---------------------|
| Stator Diameter | 30.0 mm (1.18 in) | Max Continuous Current | 45 Amps |
| Stator Thickness | 20 mm (0.79 in) | Max Continuous Power | 780 Watts |
| No. of Stator Arms | 12 | Weight | 166 Grams (5.86 oz) |
| Magnet Poles | 14 | Outside Diameter | 37.50 mm (1.47 in) |
| Motor Wind | 10 Turn Delta | Shaft Diameter | 4.98 mm (0.196 in) |
| Motor Wire | 14-Strand 0.25mm | Body Length | 45.75 mm (1.80 in) |
| Motor Kv | 890 RPM / Volt | Overall Shaft Length | 74.5 mm (2.93 in) |
| No-Load Current (I0/10V) | 1.42 Amps | Max Lipo Cell | 5s |
| Motor Resistance (Rm) | 0.020 Ohms | Motor Timing | 5deg |

Figure 33: Scorpion SII-3020-890KV-(V2) Motor Specifications

only available for upto 180 seconds. The average power available at all times still remains greater than the required power while weighing just 155 grams. Hence, this powerplant is the ideal choice for the UAV.

5.6.2 Propellers

A set of 2-blade propellers compatible with the selected motor was chosen from the catalog of the company - KDE Direct®. These propellers are made out of carbon fibre and are dynamically balanced for smooth, vibration-free operation. Each propeller has a diameter of 12.5 cm and pitch of 4.3 as seen in Fig. 32. When coupled with the above motor, these propellers can produce upto 47.898 N each at 13412 RPm and 95.8 N in total.

5.6.3 Electronic speed controller

Electronic speed controllers is one of the important part responsible for the desired performance and stability of the UAV. The Scorpion Tribunus 06-120A (SBEC) speed controller was chosen to match the scorpion motor. This has inbuilt fully integrated air telemetry module and can be programmed from the radio and has a stored battery eliminator circuit.

5.6.4 Battery

To power the selected motors, four sets of 6750 mAh Lithium Polymer batteries were used. Each battery weighs 605 grams and has an operating voltage of 14.5 V which is the same as the operating range of the motors. Detailed specifications of the battery can be seen in Fig. 36 and Fig. 37.



Figure 34: KDE direct propellers



Figure 35: Scorpion Tribunus 06-120A (SBEC) ESC



Figure 36: Tattu® 6750 mAh LiPo Battery

Tattu 6750mAh 4S 25C Lipo Battery Specs:

- Capacity: 6750mAh
- Voltage: 14.8V/4S
- Discharge Rate: 25C
- Weight: 605g
- Size: 135X42X44mm
- Charge Rate: 1-3C Recommended, 5C Max

Figure 37: Battery Specifications

5.7 Tail sizing

The empennage part of the aircraft or in this case the UAV , are modelled so as to provide dynamic stability to the vehicle. Here the conventional tail is considered for the purpose of aerodynamic and manufacturing simplicity. The tail sizing is an iterative process as it initially requires information about the location of centre of gravity of the entire UAV, the shift in CG during various flight maneuvers (CG Excursion) and the stability of the aircraft in the cruising conditions (trimmability of the aircraft). But all these in turn require accurate data about tail sizing, eventually forming a paradox.

Hence the sizing was carried out using the methods suggested in the Gudmundson book.[8] which proved to be helpful. This method makes use of the vertical and horizontal tail volumes. These non-dimensional ratios as said in the Gudmundson book compare the product of the planform area of the horizontal or vertical stabilizer and their distance from the main lifting surface (main wing) geometry, which is the product of either the mean aerodynamic chord and wing area or the wing span and wing area. Tail arm is assumed to be around 50-55 pc of the total fuselage length. this is the distance between the centre of gravity of the airplane and the mean aerodynamic centre of the horizontal and vertical tail wing respectively.

This distance is of greater importance as this distance increases the overall weight of the structure decreases , as the size of the empennage would be reduced. The main function of this tail arm is to counteract the pitching moment that is created by the main wing.

$$V_{HT} = (l_{HT}.S_{HT})/(C_{ref}.S_{ref}) \quad (15)$$

$$V_{VT} = (l_{VT}.S_{VT})/(b_{ref}.S_{ref}) \quad (16)$$

Some other important assumptions made for the tail sizing from the historical and statistical data provided for the general aviation twin engine aircraft in the Gudmundson book are presented in the table below.

General aviation aircraft

| | |
|------------------------------|-----------|
| Wing taper ratio | 0.3 - 10 |
| Wing aspect ratio | 6 - 11 |
| Horizontal tail aspect ratio | 3 - 6 |
| Horizontal tail taper ratio | 0.5 - 1.0 |
| Vertical tail aspect ratio | 0.5 - 1.0 |
| Vertical tail taper ratio | 1 - 4 |

Figure 38: Empirical data from the Gudmundson book

The volume coefficients of horizontal and vertical tails are however again estimated from the empirical data provided in the fixed wing unmanned aircraft systems database.[10] The horizontal tail volume coefficient is taken as 0.8 and vertical tail volume coefficient is taken as 0.07.

Using the above mentioned formulae and assumptions the tail sizing was done and the values extracted from this study are shown in the table below

| Parameters | Horizontal tail | Vertical tail |
|--------------|-----------------------|-----------------------|
| Taper ratio | 0.6 | 0.6 |
| Aspect ratio | 6 | 4 |
| Span | 0.907 m | 0.621 m |
| Wing area | 0.1312 m ² | 0.0965 m ² |
| Root chord | 0.188 m | 0.1942 m |
| Tip chord | 0.1132 m | 0.1165 m |

Figure 39: Assumed parameters for the present UAV

5.8 Aerodynamic centre, Neutral point and CoG estimation

The longitudinal center of gravity is defined as the point in space where the uniform force acting on the whole system is equivalent to a point force on that particular point. It could also be interpreted as the balancing point of an object, where the object stays in equilibrium.

The longitudinal center of gravity of the aircraft is estimated by considering the aircraft as a single line as the aircraft is symmetrical along the x-axis when viewed from top view. And the components of the aircraft were manually placed to get the desired overall CG of the aircraft to be around 40% of the fuselage length, thus making it a nose heavy aircraft. Along the Y-axis direction for the purpose of simplification, symmetry was implemented so that there's very minute CoG shift in the Y-direction. Also care was taken such that the CG does not shift behind the neutral point. This was an iterative process. The CG is estimated by implementing a MATLAB code with the following formula[8],

$$X_{CG} = \frac{M_X}{W_{tot}} = \frac{\sum_{i=1}^N W_i \times X_i}{W_{tot}} \quad (17)$$

where, N=number of components, W_i is the specific component weight, X_i is the location of the mass W_i on the longitudinal axis. The initial assumed values of the component location for a desired Cg can be found in the following table,

| Components | X-location (in % of total length from datum) | Fuselage length location | Weight of components (in kg) |
|-----------------------------|--|--------------------------|------------------------------|
| Main wing | 45% | 0.6570m | 1.4 |
| Horizontal stabilizer | 90% | 1.3140m | 0.62 |
| Vertical stabilizer | 85% | 1.2410m | 0.4 |
| Fuselage | 40% | 0.5840m | 1 |
| Electronic Speed Controller | 47% | 0.6862m | $0.108*2 + 0.05$ |
| Engines (with propellers) | 45% | 0.6570m | $(0.166 + 2*0.0188) *2$ |
| Battery | 28% | 0.4088m | $0.605*4$ |
| Servos (Elevators) | 91% | 1.3286m | $0.04*2$ |
| Servo (Rudder) | 91% | 1.3286m | 0.04 |
| Servos (Aileron) | 60% | 0.8760m | $0.04*2$ |
| Autopilot | 32% | 0.4672m | $0.226 + 0.05$ |
| Parachute | 40% | 0.5840m | 0.08 |
| Payload | 40% | 0.5840m | 2 |

Figure 40: Centre of gravity positions

Battery component was moved forward and aft positions in the fuselage to get the desired CG of the aircraft. Initially, CG is calculated without the payload, and the results were that the CG is located at 39.85% of the fuselage length. Hence, to balance the UAV after delivering of the payload mid air, it is decided to place the payload at 39.91 % of the fuselage length thereby avoiding the CG travel once the payload is delivered.

| | |
|------------------------|---------------|
| With payload | CG - 0.5827 m |
| After dropping payload | CG - 0.5818 m |
| CG shift | 0.0009 m |

The Aerodynamic center of the wing and the tail surfaces is determined by extending the root chord on both sides by the tip chord distance, and extending the tip chord on both sides by the root chord distance. Then, the opposite points are joined by drawing diagonals which intersect at a point, called the aerodynamic center. And on extending a line through the aerodynamic center parallel to the chord, we get the mean geometric chord of the wing and the horizontal tail surfaces. The estimation of the aerodynamic center is carried out using Solid works sketching of the wing and the tail surfaces for 1:1 scale. The aerodynamic center for the wing can be observed from Fig. 42, and a similar procedure is applied to determine the aerodynamic center of the tail surfaces.

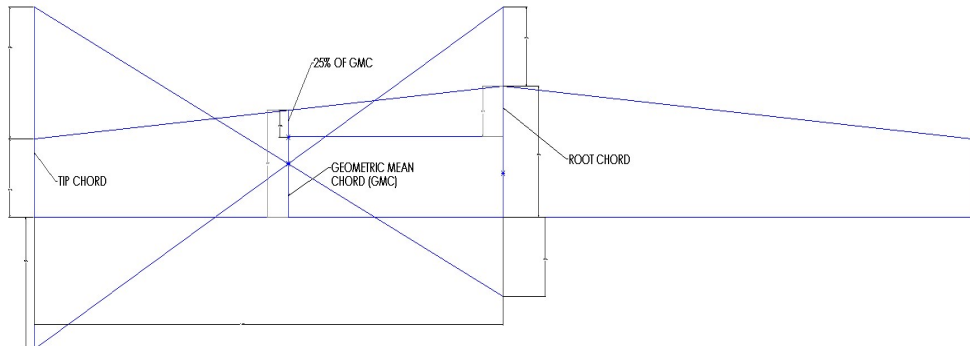


Figure 41: Aerodynamic center of the main wing

Having larger static margin would result in a UAV that would be easier to control and have greater longitudinal stability. So the optimum horizontal tail size is necessary to scale the static margin that is required for the mission. However the usual limit for the static margin lies between 5 to 15 percent.

5.9 Control surfaces sizing

Control Surfaces are used to induce Pitch, Yaw and roll effects to an aircraft. Pitch is controlled by the elevators and horizontal stabilizers, Yaw is controlled by the rudder which cumulatively comprises of the empennage as discussed earlier.

The last flight control lies on the wing responsible for roll. The ailerons are placed at the tip of the wing to achieve high roll capabilities with minimal trim.

Ailerons require symmetric Airfoils as it needs to produce both Lift and Down force based on the direction of roll. Hence, NACA 0012 was chosen for the UAV. The control surface sizing procedure contains a lot of factors and math behind it. This includes the mission of the aircraft (acrobatic or glider or training, etc), whether the control surfaces are powered or unpowered, operating altitude and speeds of the aircraft and so on. From the statistical data as shown in table43, considering our UAV to be a trainer the following relations are implemented in the sizing procedure.

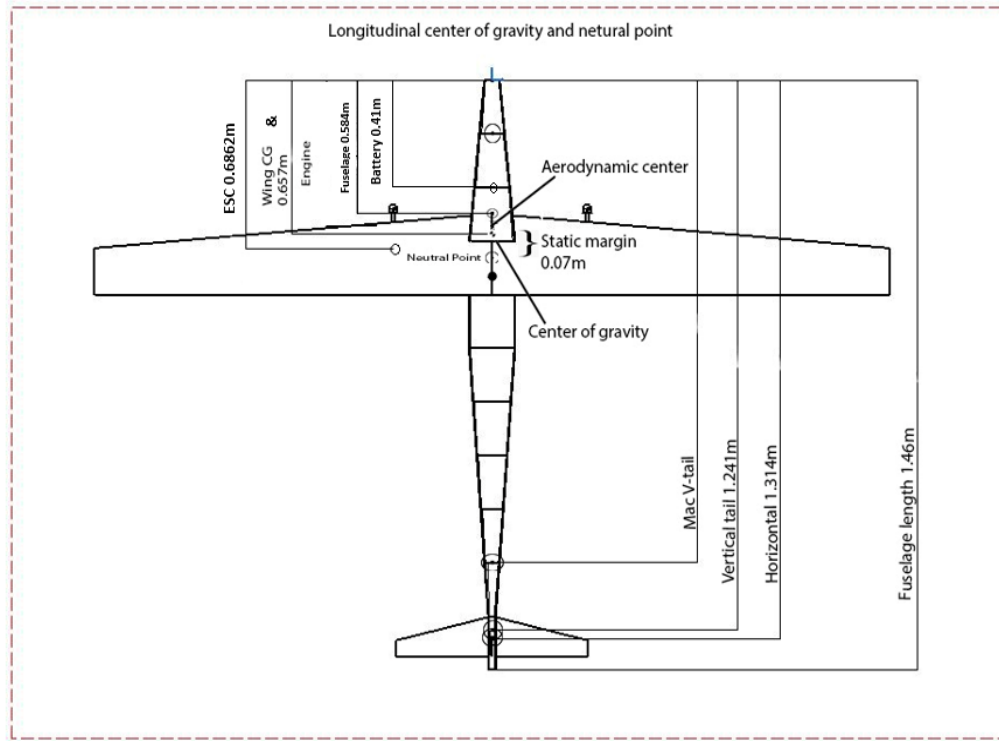


Figure 42: Overall and particular component centre of gravity location

The span of the Aileron is 0.618 m. And the deflection angles would range upto ± 20 degrees for aileron and ± 25 to 30 degrees for both rudder and elevators.

| | Elevator (% of Horizontal stabilizer) | Rudder (% of Vertical stabilizer) | Aileron (% of Main wing) |
|---------------------------|---|---|-----------------------------|
| Trainer | 20 % | 10-15 % | 20 % |
| Sport Aerobatic | 30 % | 25 % | 25 % |
| Aerobatic (non-3D) | 40 % | 30 % | 25 % |
| 3D | 60 % and above | 75 % and above | 35 % and above |

Figure 43: Control surfaces chord relations

5.10 Miscellaneous systems in the UAV

UAV is a combination of many subsystems. They include servo and actuators, electronic speed controllers, sensors, Parachute block, autopilot (flight computer), flight control board, receiver systems, flight gyro and so on.

The communication systems in the most commercial UAVs right now use HF or VHF, in absence of the on-board GPS systems. Autopilot is one of the most complex system that goes into the UAV. Since there is no manual human interference in the UAV system, autopilot has to perform all the things that a pilot would perform with the inputs received from the ground radio transmitter or a pre-stored command code.

The mechanism for payload delivery was pre-designed to be done with the help of a parachute, avoiding the need to land in the delivery location thereby reducing the turn around time and need for the landing gear. The parachute is made up of light material , (a cousin of plastic like polymer or polystyrene) ,where the weight can be as low as 400 grams.The table in Fig 44 gives the overall picture of the main components that house inside the UAV.

| Components | Names | Specifications |
|-----------------------------|--|--|
| Electric Brushless Motor | Scorpion SII-3020-890KV (V2) | Max Power: 780 watts Weight: 166 grammes Input voltage: 14.8 v Kv (Motor velocity constant): 890RPM/V |
| Battery | Tattu 6750mAh 4S 25C Lipo (four in number) | Capacity: 6750mAh Voltage: 14.8V/4S Weight: 605 grammes Discharge rate: 25C |
| Electronic Speed Controller | Scorpion Tribunus 06-120A (SBEC) | Mikado V control, Jeti telemetry Input voltage 11-26.1 volts 108 grammes |
| Propeller | KDE-CF125-DP | Propeller Blades, 12.5" x 6.3 Carbon fiber Weight: 18.8 grammes |
| Torque Servo Motor | Hitec HS-85MG Servo Motor | Speed (sec/60o): 0.13 Torque: 3.5 Kg/cm Size (mm): 29 x 13 x 30 Weight: 21.9 grammes |
| Autopilot | Arkbird 2.0 Autopilot System | Flight stabilization, autopilot and navigation system Weight: 226 grammes Return home functionality |
| Receiver | Scorpion IR Receiver | Weight: 6.9 grammes |

Figure 44: Systems and components of the UAV

5.11 Range and Endurance as a function of cruise speed

Range of an aircraft is defined as the distance an aircraft can fly for a given amount of time. The design viability of the aircraft can be determined by assessing the distance an aircraft can fly for. The range for an aircraft can be calculated by segregating the mission profile into different segments, and based on the fuel consumption of the engine it can be calculated. But since we are dealing with an battery-powered electric UAV, a separate method has been implemented here for calculating the Range of the aircraft as a function of the cruise segment[8]. Since the weight of an electrically-propelled aircraft does not change with the range, the calculation of range is to be handled differently.

For a battery-powered electric aircrafts, it is assumed that the aircraft is flying at an constant altitude, which in our case is the cruise altitude of about 4000 ft. And for this case, the suggested mission profile for the aircraft can be observed from Fig. 45.

The total battery weight, based on the selection criterion, is 2.4 kg (0.6 kg each) with an Energy Density of 200 Wh/kg.

For calculating the range for various cruise speeds, a MATLAB code is being

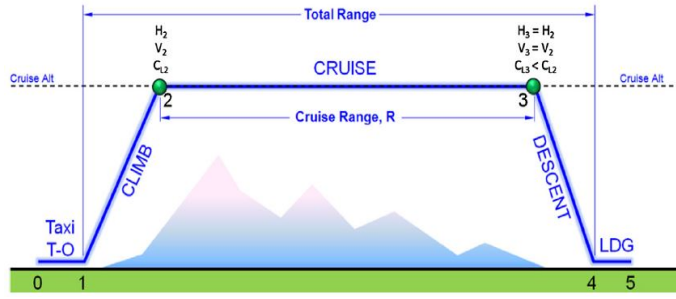


Figure 45: Suggested mission profile

implemented here to get the desired output. First the cruise velocity of the aircraft is being varied at constant altitude, and then based on the total drag force acting on the aircraft the required power is being calculated using the following equation,

$$P_{REQ} = D * V \quad (18)$$

where, D is the drag force being calculated for the particular cruise speed, and V is the cruise speed. Next step is to calculate the total amount of time required to run the motor, which in-turn gives us the Endurance for various cruise speeds, is calculated using the following formula,

$$t_{TOT} = \frac{E}{D * V} \quad (19)$$

where, E is the total energy (Wh) stored in the battery system ($E = \text{mass of the battery} * \text{Energy Density}$). Finally, the range for a particular cruise speed is being calculated using the following equation,

$$R = t_{TOT} * V \quad (20)$$

The generated plot for Range as a function of cruise speed can be observed from Fig. 46.

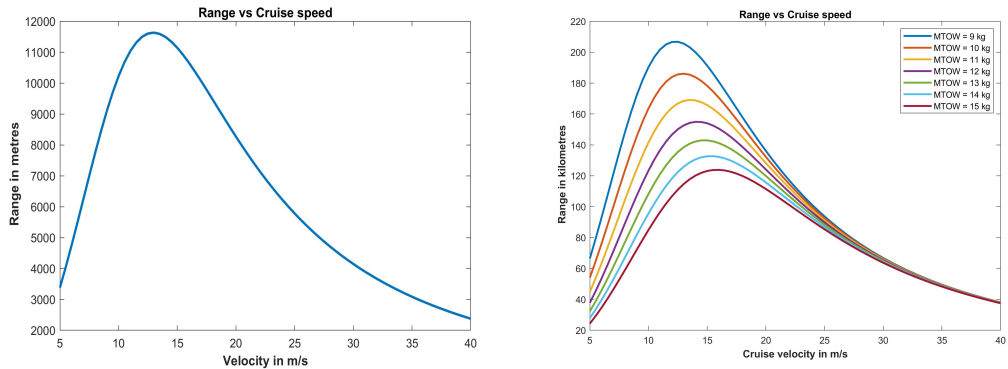


Figure 46: Range for various cruise speeds

It can be observed from Fig. 46 that a maximum range of about 11000 m can be obtained if the aircraft cruises at around 11-12 m/s, and a minimum range less than 3000 m for a cruise speed of 40 m/s. Also, a sensitivity analysis is carried out

based on the MTOW of the aircraft and can be observed from Fig. 46. Here, it can be observed that as the MTOW of the aircraft is increased, the range decreases. This may be due to the reason that a higher capacity battery would be required for a higher MTOW to sustain a long-range flight.

Similarly, the Endurance of the aircraft for various cruise speeds is obtained from the t_{TOT} calculated for the range. The calculated Endurance for various cruise speeds can be observed from Fig. 47. It can be observed that a maximum Endurance of about 2.7 hours can be attained for a cruise speed of about 12-13 m/s, while minimum endurance of less than 0.5 hours can be observed for a cruise speed of 40 m/s. Also, a sensitivity analysis has been carried out based on the MTOW of the aircraft, and can be observed from Fig. 47. It can be observed from that as the MTOW of the aircraft increases, the endurance of the aircraft decreases for the optimum cruise speed.

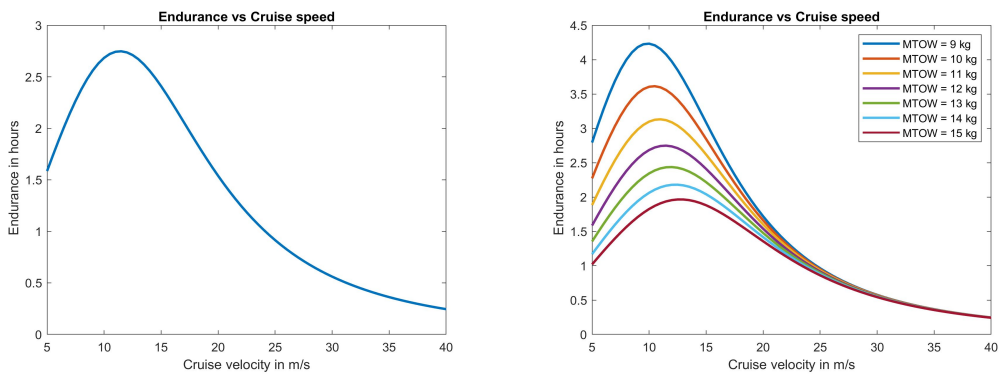


Figure 47: Endurance for various cruise speeds

5.12 Power required as a function of cruise speed

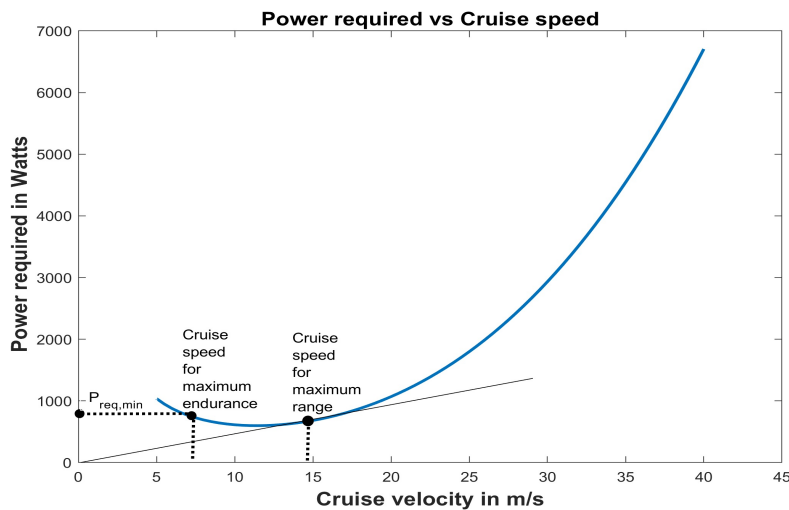


Figure 48: Power required for various cruise speed

From Fig. 48, the power requirement at various cruise speeds can be observed.

Two specific points on the curve are highlighted which indicates the required power for maximum endurance and required power for maximum range. The required power increases exponentially as the cruise speed increases beyond 25 m/s.

5.13 Drag Polar

The component of the aerodynamic force acting in the direction parallel to the wind direction is known as the Drag force. The total drag acting on the aircraft is divided into two components, namely, Parasitic Drag and Lift-Induced Drag. A MATLAB code has been implemented here to calculate the total drag acting on the aircraft. First, the aircraft is divided into geometrical bodies like fuselage, wing, pylon, nacelle, horizontal tail and vertical tail, and a component-wise drag-breakdown is being calculated using the form factors for each component, and hence the total parasitic drag C_{D0} is calculated. Next, the total drag coefficient is calculated using the following equation,

$$C_D = C_{D0} + C_{Di} = C_{D0} + \frac{C_L^2}{\rho \pi A} \quad (21)$$

Thus, the obtained Drag Polar for various aircraft speeds can be observed from Fig. 49.

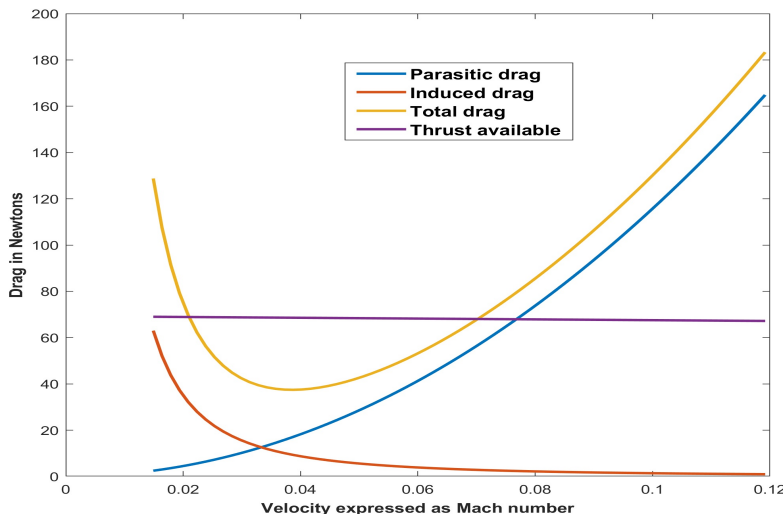


Figure 49: Drag Polar

It can be observed from Fig. 49 that the lift-induced drag is higher during the take-off phase, since higher lift is required for lift-off, thereby producing higher lift-induced drag. With the increase in speed, a drastic increase in the parasitic drag is observed since the air is moving over the body with much higher velocity, thereby creating higher friction drag contributing to the parasitic drag produced. The available static thrust to the aircraft is the thrust produced by the motors, which remains almost constant throughout the flight. The area between the static thrust line and the total drag curve defines the excess thrust available to the aircraft by overcoming the drag.

A sensitivity analysis is performed here to check the excess thrust available to the aircraft by varying the flight altitude, and the results are checked for 2 different altitudes - 2000 ft and 8000 ft. It was observed that as the flight altitude is increased, the thrust available to the aircraft decreases.

5.14 Specific Excess Power

Excess power can be defined as the difference between the available power and the required power for an aircraft. SEP provides a contour with the rate of excess power as a function of altitude. Fig. 50 shows the untrimmed SEP contour without any operating restrictions for the UAV. Here, it can be observed that when the UAV is flying at the cruise altitude (around 1.2 km), a specific excess power of 5 m/s is still left even after completing the mission.

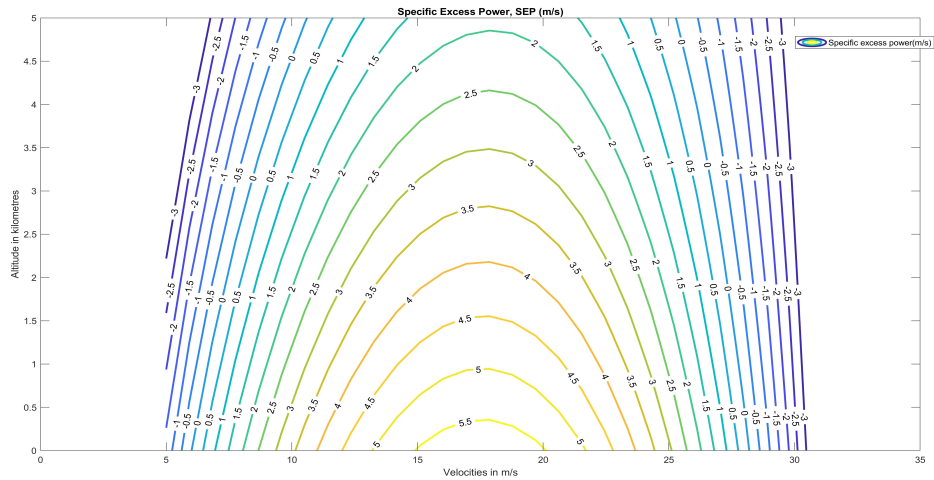


Figure 50: SEP Contour Plot

5.15 V-n Diagram

Fig. 51 shows the V-n diagram with a designated safe operating envelope for the load factor as a function of speed.

5.16 Parachute Sizing

Parachutes are used for two purposes in the UAV. The payload container is mounted to a parachute in order to safely deliver the payload at the destination. Since the payload has an upper limit of 2 kgs, the parachute is designed appropriately based on the velocity of descent. If the payload is very sensitive, then a lower velocity of descent is appropriate and a higher velocity of descent can be chosen for payloads which can withstand a round landing. The radius of the parachutes with different velocities of descent can be seen in Fig. 52

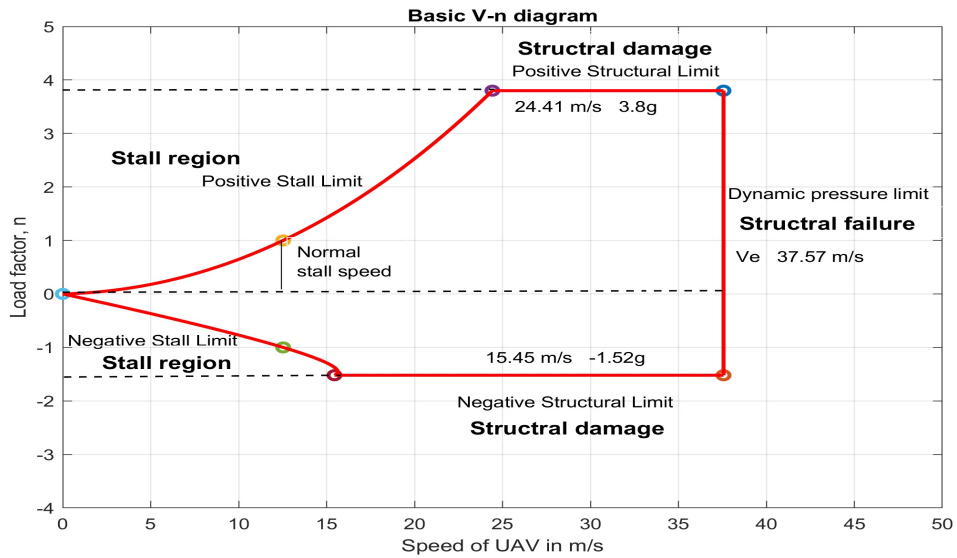


Figure 51: V-n Diagram

| Velocity of Descent | Radius of the Parachute |
|---------------------|-------------------------|
| 4 m/s | 0.728 m |
| 5 m/s | 0.582 m |
| 6 m/s | 0.485 |

Figure 52: Payload Parachute Sizing

The second parachute is used as a secondary recovery system for the UAV in case belly landing is not feasible. The weight of the UAV will be 7.4 kgs without the payload. Hence Fig. 53 shows the radius of parachutes with different velocities of descent.

| Velocity of Descent | Radius of the Parachute |
|---------------------|-------------------------|
| 2 m/s | 2.355 m |
| 1 m/s | 4.71 m |

Figure 53: UAV Recovery Parachute Sizing

6 Final Results

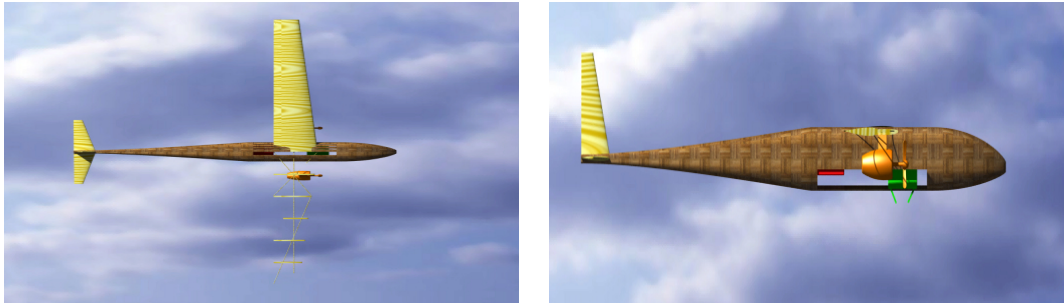


Figure 54: Top view and Side View of the UAV

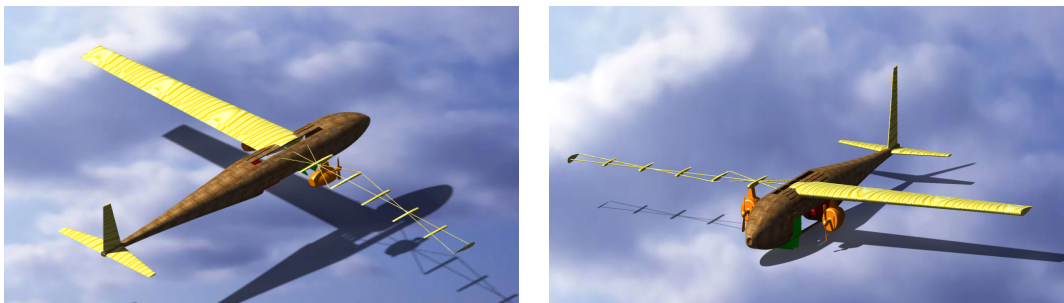


Figure 55: Isometric Views of the UAV

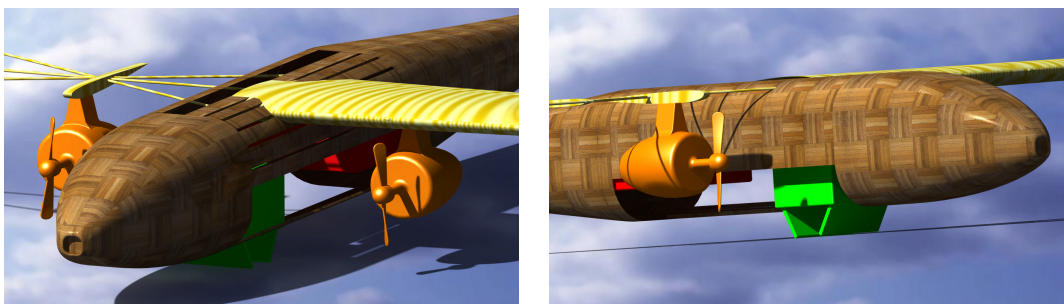


Figure 56: Payload Container, Battery Box and Engine detailed view

Figures 54, 55 and 56 shows the various views of the UAV. It can be seen that half of the UAV wing is hidden such that the wing spars are visible. The portion of the fuselage is also hidden such that the Payload container and the battery box is visible. The wing spars are connected to the ribs of the fuselage. One wing spar runs from the root to tip to provide overall structural stability and to withstand bending loads. Diagonal spars ensure stability against torsional loads. Since, the UAV is launched using a catapult, the rate of acceleration is fairly high which creates a whiplash effect on the wing. These spars help to maintain structural integrity. The UAV is designed with Balsa wood which is known for it's light weight and easy manufacturability.

It can be seen that the payload box is placed strategically placed in the Fuselage. By placing the box at the position of CoG at 0.5869 m, a minimal CG travel of 0.0004 m can be ensured after dropping the payload. This leads to stable flight conditions with/without the payload.

Fig. 57 shows the detailed breakdown of the dimensions are geometrical data of each component.

| Parameter | Value |
|-----------------|-----------------------|
| Wing Span | 2.1 m |
| Wing Area | 0.5521 m ² |
| Wing root chord | 0.2561 m |
| Wing tip chord | 0.1536 m |
| Wing AR | 8 |
| Wing MAC | 0.2091 m |
| HT Span | 0.907 m |
| HT Root Chord | 0.188 m |
| HT Tip Chord | 0.1132 m |
| HT AR | 6 |
| VT Span | 0.621 m |
| VT Root Chord | 0.1942 m |
| VT Tip Chord | 0.1165 m |
| VT AR | 4 |
| Fuselage Length | 1.46 m |
| Fuselage Width | 0.224 m |
| Fuselage Height | 0.25 m |

Figure 57: UAV Dimensions

7 Discussion and Conclusion

A fully functional UAV has been designed which meets the initial requirements. A lot of design changes and improvements were made to the initial ideas to meet reality. Most design innovations like V-tail, blended wings etc., were ruled out because of excessive disadvantages. The final design consists of a simple, practical, conventional aircraft focusing on the cause it has been built for. However, the integration of metallic components like engines, battery to the non-metallic balsa wood still remains as an area for research. Alternative materials might have to be chosen in the future to assure durability of the UAV. The absence of landing gears make the UAV prone to hard impacts even with the fail-proof dual landing mechanisms. Since detailed structural analysis was not performed, it will be a major scope for improvement. And when carefully seen with the eyes of an experienced aircraft designer it can be said that the UAV has a fuselage which is of no use here. So instead of the fuselage presented in the CAD models, a reduced fuselage that is almost 50 to 60% of the current length of the fuselage with a boom of 30 to 40% of fuselage length will be integrated. Due to the time constraints this part is left out. Since we have already have the MATLAB codes for weight estimations and CoG locations, only designing on CATIA will be the major work involved here.

References

- [1] LR N. Unmanned Aviation: A Brief History of Unmanned Aerial Vehicles. Reston, VA: American Institute of Aero-nautics and Astronautics; 2004. https://www.researchgate.net/publication/328480646_Surgical_and_Medical_Applications_of_Drones_A_Comprehensive_Review.
- [2] Mwanza RC. The use of unmanned aerial vehicles for health purposes: a systematic review of experimental studies; 2018. <https://www.ncbi.nlm.nih.gov/pmc/articles/PMC6152489/>.
- [3] Tanzania G. Lake Victoria Challenge; 2019. <https://www.lakevictoriachallenge.org/competition/#emergency-delivery/>.
- [4] Jagannathan AT. Design and development of a hybrid UAV, Brunel university; 2018. <https://www.slideshare.net/CamiloVergara1/design-and-development-of-a-hybrid-uav>.
- [5] Moultrie J. Morphological charts, University of Cambridge; 2019. <https://www.ifm.eng.cam.ac.uk/research/dmg/tools-and-techniques/morphological-charts/>.
- [6] Svahn C. Quantified Interactive Morphological Matrix An automated approach to aircraft fuel system synthesis; 2019. <https://www.diva-portal.org/smash/get/diva2:22707/FULLTEXT01.pdf>.
- [7] Tech UP. Eli – Pneumatic UAV Launcher, Parachute Release Mechanism;. <http://uavpropulsiontech.com/eli-airborne-systems/>.
- [8] Gudmundson S. General Aviation Aircraft Design: Applied Methods and Procedures. 1st ed. Elsevier Inc.; 2014.
- [9] Esteban HIDALGO DIAZ O Victor Calle. Methodology for Weight and Performance Assessment of an UAV for Precision Agriculture at Cruise Condition; 2017. https://www.researchgate.net/publication/318295246_Methodology_for_Weight_and_Performance_Assessment_of_an_UAV_for_Precision_Agriculture_at_Cruise_Condition.
- [10] Palmer JL. Assembly and Initial Analysis of a Database of the Characteristics of Fixed-Wing Unmanned Aircraft Systems;. <https://apps.dtic.mil/dtic/tr/fulltext/u2/a623605.pdf>.